Newton

Article

Perturbing scattering resonances in non-Hermitian systems: A generalized Wigner-Smith operator formulation

Graphical abstract

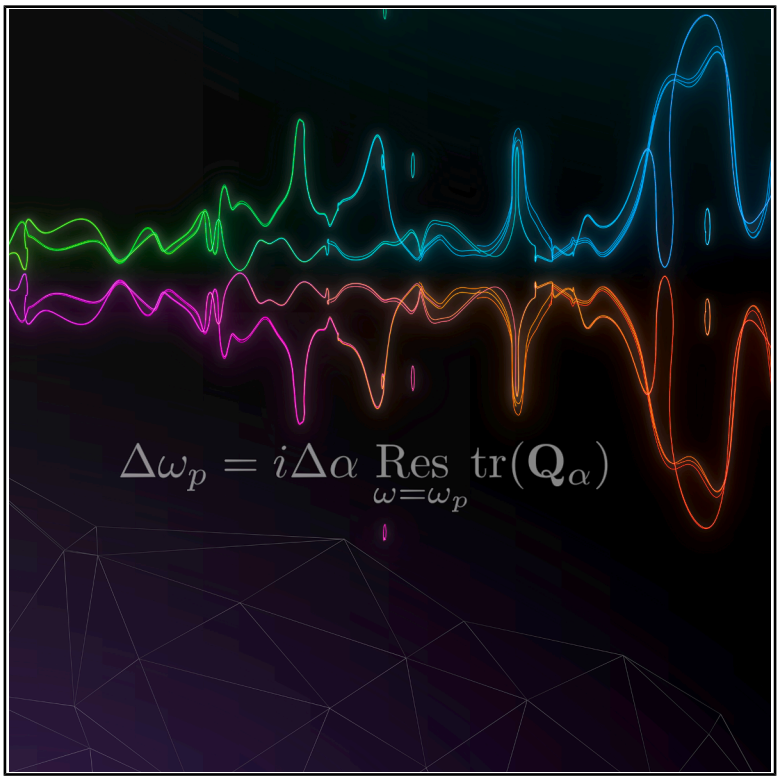

Highlights

- Analytic formula for resonance shifts using generalized Wigner-Smith operators
- Electromagnetic theory linking new results to classic perturbation theory
- Simulations of resonance shifts in perturbed complex photonic networks
- Application to selective pumping schemes in a random network laser

Authors

Niall Byrnes, Matthew R. Foreman

Correspondence

matthew.foreman@ntu.edu.sg

In brief

Understanding resonance shifts due to system perturbations in open systems requires going beyond traditional perturbation theories. Byrnes and Foreman introduce a complex-analytic perturbation formula to predict shifts in complex resonance frequencies of general resonant systems caused by arbitrary perturbations. The result, expressed in terms of generalized Wigner-Smith operators, reduces to traditional cavity perturbation theory through energetic considerations under suitable approximations. The approach is validated through simulations of perturbations to random photonic networks, including an investigation of optimal spatial pumping schemes to achieve lasing at targeted frequencies.

Byrnes & Foreman, 2025, Newton *1*, 100194
September 8, 2025
https://doi.org/10.1016/j.newton.2025.100194

CellPress

Newton

CellPress
OPEN ACCESS

Article

Perturbing scattering resonances in non-Hermitian systems: A generalized Wigner-Smith operator formulation

Niall Byrnes[1] and Matthew R. Foreman[1,2,3,*]
[1]School of Electrical and Electronic Engineering, Nanyang Technological University, 50 Nanyang Avenue, Singapore 639798, Singapore
[2]Institute for Digital Molecular Analytics and Science, 59 Nanyang Drive, Singapore 636921, Singapore
[3]Lead contact
*Correspondence: matthew.foreman@ntu.edu.sg
https://doi.org/10.1016/j.newton.2025.100194

ACCESSIBLE OVERVIEW Perturbations to resonant photonic systems cause changes in both the frequencies and linewidths of their resonant modes. These changes are conveniently captured by the motion of poles of the analytically continued scattering matrix in the complex plane as the system is perturbed. Understanding the dynamics of these shifts—particularly their sensitivity to perturbations—is critical for the design and optimization of nano-resonators, which have applications in sensing, targeted energy deposition, enhanced nonlinear optical processes, and the development of compact, high-performance lasers. In this work, we develop a complex-analytic formula to predict the shift in complex resonance frequencies resulting from arbitrary system perturbations, expressed in terms of generalized Wigner-Smith operators associated with the perturbation parameters. We further demonstrate how this formula connects to traditional electromagnetic cavity perturbation theory through energy conservation considerations under suitable approximations. Our results are validated by numerical simulations of perturbations in random photonic networks that support complex resonances. Additionally, we apply our formula to investigate optimal pumping schemes for frequency-targeted lasing in a random photonic network laser.

SUMMARY

Resonances of open non-Hermitian systems are associated with the poles of the system's scattering matrix. Perturbations of the system cause these poles to shift in the complex frequency plane. In this work, we introduce a novel method for calculating shifts in scattering matrix poles using generalized Wigner-Smith operators. We link our method to traditional cavity perturbation theory and validate its effectiveness through application to complex photonic networks and selective pumping of random lasers. Our findings underscore the versatility of generalized Wigner-Smith operators in analyzing a broad spectrum of resonant systems and provide new insight into the resonant properties of non-Hermitian systems.

INTRODUCTION

Resonance is a fundamental physical phenomenon that plays a key role in fields as diverse as quantum mechanics,[1] structural engineering,[2] electromagnetics,[3] and fluid dynamics.[4] In closed systems, resonances are associated with normal modes, which correspond to the orthogonal eigenvectors of the system's Hermitian Hamiltonian. The corresponding real eigenvalues define the spectrum of permissible oscillation frequencies or energy levels.[5] Eigenvalue problems, however, generally do not admit closed-form analytical solutions, and numerical solvers are frequently employed.[6] An alternative approach involves modeling a system as a perturbation to a solvable reference problem. Of this latter class of methods, Rayleigh-Schrödinger perturbation theory, in which the perturbed solution is written as a series expansion over all unperturbed eigenstates, is perhaps the most famous approach.[7] A multitude of alternate theories, however, have been developed, such as Brillouin-Wigner, many-body, and lattice perturbation theory.[8–10]

Although closed systems are useful theoretical ideals, in reality a system interacts with its environment. The coupling of normal modes to external degrees of freedom introduces potential loss channels, which can alter the nature and energy of resonant modes. So-called open, or scattering, systems can no longer be described by a Hermitian Hamiltonian, and a coupling operator must be introduced to form an effective non-Hermitian

Please cite this article in press as: Byrnes and Foreman, Perturbing scattering resonances in non-Hermitian systems: A generalized Wigner-Smith operator formulation, Newton (2025), https://doi.org/10.1016/j.newton.2025.100194

Hamiltonian.[11] Alternatively, one can use the closely related scattering matrix, **S**, which derives from the resolvent of the effective Hamiltonian.[12] The resonant states of the system, now termed *quasi*-normal modes (QNMs), are then identified from the poles of **S** when analytically continued into the complex frequency plane.[5,13] Notably, loss pushes the resonant frequencies off the real axis, resulting in complex-valued eigenfrequencies ω_p, where $\mathrm{Re}(\omega_p)$ and $-\mathrm{Im}(\omega_p)/2$ are the resonant frequency and linewidth.

Open systems are known to possess a number of interesting resonant and scattering phenomena, such as coherent perfect absorption,[14] exceptional points,[15] and bound states in the continuum.[16] Moreover, resonances in open systems are susceptible to environmental variations, such as changes in temperature, external fields, or material composition, a concept underpinning modern sensors.[17–19] Perturbed non-Hermitian systems can exhibit additional unique behavior, such as anomalous resonance shifts[20,21] and nonlinear sensitivity.[22] Evaluation of resonant modes and their properties therefore remains an important task in, for example, evaluating state lifetimes, laser dynamics, and sensor sensitivity. Traditional perturbation theories, however, are not directly applicable to open systems due to mathematical complexities introduced by QNMs.[23,24] For high-quality-factor resonances, such as those supported by optical microcavities,[25] coupling to the environment is weak, allowing resonance shifts to be expressed as changes in stored energy.[26,27] The validity of such expressions is, however, limited, and they fail to correctly predict changes in linewidths,[28] which is now understood to be a signature of the non-orthogonality of QNMs.[29,30] In the presence of significant losses, more careful consideration of the normalization of QNMs[28] or alternative mode expansions[31] become necessary.

In this paper, we present a novel formulation for determining resonance shifts due to arbitrary system perturbations based on generalized Wigner-Smith (WS) operators. We link our WS approach to Hamiltonian perturbation theory, illustrating how perturbations to the Hamiltonian are encoded in fields scattered away from the system. We also show that, in the case of high-quality-factor resonances, our WS approach recovers the traditional energetic resonance shift formula. Finally, we test our theory against numerical simulations of resonant scattering in random photonic networks. In an accompanying paper[32], we apply our theory to low-quality-factor resonances and present further generalizations, applications, and numerical examples.

RESULTS

Perturbation theory

An important tool commonly employed in the analysis of scattering systems is the WS time delay matrix

$$\mathbf{Q}_\omega = -i\mathbf{S}^{-1}\partial_\omega\mathbf{S}, \qquad \text{(Equation 1)}$$

where ∂_ω denotes the partial derivative with respect to frequency ω.[33,34] $\mathbf{Q}_\omega$ has several interesting properties relevant to resonant scattering. For unitary systems at real ω, $\mathbf{Q}_\omega$ is Hermitian, and its eigenvalues are associated with well-defined time delays experienced by narrow-band, transient system excitations. Evaluated at scattering matrix poles, these time delays coincide with the lifetimes of the associated resonances, demonstrating a link between $\mathbf{Q}_\omega$ and a system's QNMs.[35] In electromagnetic theory, it has also been shown that diagonal elements of $\mathbf{Q}_\omega$ can be expressed as energy-like integrals over the extent of the system,[36] highlighting the connection to mode volume.

By itself, $\mathbf{Q}_\omega$ lacks the specificity required to efficiently capture localized or parametric system perturbations. For this reason, we also consider the generalized WS operator $\mathbf{Q}_\alpha$, defined by Equation 1 with $\omega \to \alpha$, where α is an arbitrary variable. Operators of this kind have recently attracted attention in the optical domain as a tool for designing systems and engineering light in complex scattering environments.[37–40] Importantly, by virtue of its generalized nature, $\mathbf{Q}_\alpha$ contains sufficient information to predict resonance shifts induced by arbitrary system perturbations. To show this, we consider a generic scattering system described by a scattering matrix **S**, whose poles are assumed to be of order one. Let α (α') denote some system parameter, such as the temperature, shape, or size of some component of the system, before (after) it is perturbed. To determine the change in the resonant frequency $\Delta\omega_p = \omega_p' - \omega_p$ that is induced by the perturbation $\Delta\alpha = \alpha' - \alpha$, we consider the function $f(\omega, \alpha) = \det[\mathbf{S}^{-1}(\omega, \alpha)]$, whose zeros coincide with the poles of **S**. Assuming the perturbation is small, a first-order, multivariate Taylor expansion of f gives

$$f' = f + (\omega' - \omega)\partial_\omega f + (\alpha' - \alpha)\partial_\alpha f, \qquad \text{(Equation 2)}$$

where $f = f(\omega, \alpha)$ and $f' = f(\omega', \alpha')$. Ideally, we would evaluate Equation 2 at $\omega = \omega_p$ and $\omega' = \omega_p'$ and solve for $\Delta\omega_p$. Some care is required, however, in recasting the result back in terms of **S**, whose elements diverge at ω_p. This problem can be mitigated using residue calculus, which ultimately yields (see methods for more details)

$$\Delta\omega_p = i\Delta\alpha \operatorname*{Res}_{\omega=\omega_p} \mathrm{tr}(\mathbf{Q}_\alpha) = -\Delta\alpha \frac{\mathrm{Res}_{\omega=\omega_p}\mathrm{tr}(\mathbf{Q}_\alpha)}{\mathrm{Res}_{\omega=\omega_p}\mathrm{tr}(\mathbf{Q}_\omega)}, \qquad \text{(Equation 3)}$$

where tr denotes the trace operator and $\mathrm{Res}_{\omega=\omega_p}$ denotes the residue at the pole ω_p. As can be seen from Equation 3, for a given perturbation $\Delta\alpha$, the pole shift $\Delta\omega_p$ is completely determined by $\mathrm{Res}_{\omega=\omega_p}\mathrm{tr}(\mathbf{Q}_\alpha)$, which should be evaluated for the *unperturbed* system. We also observe that the form of Equation 3 implies that the ratio of the residues of the generalized WS operators behaves as a condition number for ω_p when treated as a function of α.[41] Equation 3 is our key result, which, importantly, was derived on purely mathematical grounds and is therefore applicable to a broad range of physical scenarios. We note that our complex-analytic approach has conceptual links to a recently developed method involving Riesz projections.[42] In Binkowski et al.,[42] the pole shift is obtained by

Please cite this article in press as: Byrnes and Foreman, Perturbing scattering resonances in non-Hermitian systems: A generalized Wigner-Smith operator formulation, Newton (2025), https://doi.org/10.1016/j.newton.2025.100194

finding residues of linear functionals of the electric field, calculated using a direct differentiation method. In contrast, our approach assumes knowledge of the scattering matrix, which, as will be demonstrated, provides additional conceptual links to other aspects of scattering theory and non-Hermitian physics.

Connection to Hamiltonian-based perturbation theory

Traditional perturbation theory is typically expressed in terms of changes to the system's Hamiltonian, the eigenvalues of which correspond to resonant frequencies. To illustrate the relationship between this framework and our perturbation formula, we consider a toy example: a closed cavity supporting a single resonant mode with real eigenfrequency ω_0. If the system is exposed to the environment by a collection of N scattering channels, then the system's $N \times N$ scattering matrix can be written as[43]

$$\mathbf{S} = \mathbf{I} - \frac{2i\mathbf{u}\mathbf{u}^\dagger}{\omega - \omega_0 + i\mathbf{u}^\dagger\mathbf{u}}, \qquad \text{(Equation 4)}$$

where $\mathbf{I}$ is the $N \times N$ identity matrix and $\mathbf{u}$ is a vector of N coupling coefficients, assumed to be independent of frequency. Evidently, coupling to the environment shifts the resonant frequency off the real axis, giving rise to a QNM with complex resonant frequency $\omega_p = \omega_0 - i\mathbf{u}^\dagger\mathbf{u}$.

We can find $\mathbf{Q}_\alpha = -i\mathbf{S}^{-1}\partial_\alpha\mathbf{S}$ by differentiating Equation 4 and noting that $\mathbf{S}^{-1}$ is given by the same expression as in Equation 4 but with the replacement $i \to -i$. After some algebra, we obtain

$$\mathrm{tr}(\mathbf{Q}_\alpha) = i\frac{\partial_\alpha(\omega - \omega_p)}{\omega - \omega_p} + \frac{a}{(\omega - \omega_p)^2} + \frac{b}{\omega - \omega_p^*}, \qquad \text{(Equation 5)}$$

where a and b are factors independent of ω. Equation 5 is essentially a Laurent series, from which the residue at the pole ω_p can be readily extracted, giving $\mathrm{Res}_{\omega=\omega_p}\mathrm{tr}(\mathbf{Q}_\alpha) = -i\partial_\alpha\omega_p$. Finally, the approximation $\partial_\alpha\omega_p \approx \Delta\omega_p/\Delta\alpha$ yields Equation 3. It can thus be seen that the meromorphic structure of $\mathrm{tr}(\mathbf{Q}_\alpha)$ is such that the change in the system's resonant frequency (i.e., $\partial_\alpha\omega_p$) manifests as the residue at the associated pole. In our example, $\omega_0 - i\mathbf{u}^\dagger\mathbf{u}$ is the system's scalar effective Hamiltonian. For systems possessing multiple resonant modes, the inverse factor in Equation 4 is instead expressed as the resolvent $(\omega\mathbf{I} - \mathbf{H}_{\mathrm{eff}})^{-1}$ of an effective Hamiltonian matrix $\mathbf{H}_{\mathrm{eff}}$. In this case, Equation 5 would take the form of a more general pole expansion, summed over the different resonant frequencies of the system.[44] Taking the residue of $\mathrm{tr}(\mathbf{Q}_\alpha)$ at a particular pole, however, ultimately yields the corresponding resonance shift. Notably, while traditionally the frequency shift is given by the inner product $\psi^\dagger\Delta\mathbf{H}\psi$, where ψ is the resonant mode of the unperturbed system, the use of the trace operator in Equation 5 effectively isolates the single diverging eigenvalue of $\mathbf{Q}_\alpha$ at ω_p. The resonance shift is thereby determined directly from the scattering matrix without requiring knowledge of the system's internal modes. This makes our approach particularly useful for systems for which a scattering matrix formalism is most natural.

Connection to electromagnetic theory

Having discussed WS operators more generally, we now relate our approach to classical electromagnetic theory. To gain physical insight into Equation 3, we consider a class of optical systems composed of arbitrary, finite interior regions coupled to the environment by a finite number of dielectric waveguides. Examples of such systems include fiber Bragg resonators, complex networks, and ring resonators.[45–47] Note that Equation 3 can be written in the form

$$\Delta\omega_p = \lim_{\omega\to\omega_p}\left[-\Delta\alpha\frac{\mathrm{tr}(\mathbf{Q}_\alpha)}{\mathrm{tr}(\mathbf{Q}_\omega)}\right], \qquad \text{(Equation 6)}$$

and so the pole shift is given approximately by the expression within the limit evaluated at $\omega \approx \omega_p$. We assume for simplicity that the system permittivity ϵ is real and isotropic and that the permeability μ_0 is that of free space. Restricting to resonances with high quality factors such that $\mathrm{Im}(\omega) \ll \mathrm{Re}(\omega)$, it is possible to show on the basis of energy conservation that (see methods for more information)

$$\mathbf{Q}_\xi = \left[\mathbf{I} + 2\mathrm{Im}(\omega)\int_\Omega(\epsilon\mathbf{U}^e + \mu_0\mathbf{U}^m)\,dV\right]^{-1} \left[-\int_\Omega\left[\partial_\xi(\omega\epsilon)\mathbf{U}^e + \partial_\xi\omega\mu_0\mathbf{U}^m + 2i\mathrm{Im}(\omega)\left(\epsilon\mathbf{V}_\xi^e + \mu_0\mathbf{V}_\xi^m\right)\right]dV\right], \qquad \text{(Equation 7)}$$

where ξ represents either ω or α and Ω denotes the volume occupied by the system with a boundary $\partial\Omega$ perforated only by the coupling waveguides. In Equation 7, $\mathbf{I}$ is the identity matrix, and $\mathbf{U}^e, \mathbf{U}^m, \mathbf{V}_\xi^e$, and $\mathbf{V}_\xi^m$ are matrices whose (q,p)-th elements are given by $U_{qp}^e = \frac{1}{4}\mathbf{E}_p\cdot\mathbf{E}_q^*$, $U_{qp}^m = \frac{1}{4}\mathbf{H}_p\cdot\mathbf{H}_q^*$, $V_{\xi,qp}^e = \frac{1}{4}\partial_\xi\mathbf{E}_p\cdot\mathbf{E}_q^*$, and $V_{\xi,qp}^m = \frac{1}{4}\partial_\xi\mathbf{H}_p\cdot\mathbf{H}_q^*$ respectively, where the fields $\mathbf{E}_p$ and $\mathbf{H}_p$ ($\mathbf{E}_q$ and $\mathbf{H}_q$) are those that exist throughout Ω when the system is illuminated by the p-th (q-th) incident field. Here, p and q enumerate all modes in all waveguides that couple the system to the environment.

The form of $\mathbf{Q}_\xi$ in Equation 7 reflects the factorization, $\mathbf{Q}_\xi = \mathbf{A}^{-1}\mathbf{B}_\xi$, where $\mathbf{A} = \mathbf{S}^\dagger\mathbf{S}$ and $\mathbf{B}_\xi = -i\mathbf{S}^\dagger\partial_\xi\mathbf{S}$. Physically, the diagonal entries of $\mathbf{A}$ describe the energy flux through the system's boundary, while those of $\mathbf{B}_\omega$ quantify the stored electromagnetic energy within the system. The product $\mathbf{A}^{-1}\mathbf{B}_\omega$ can thus be interpreted as a multichannel generalization of the dwell time operator, traditionally defined as the ratio of stored energy to outgoing flux.[35] The diagonal elements of the matrix $\mathbf{B}_\alpha$, on the other hand, by virtue of the α derivatives, can be understood as describing changes in energy induced by the perturbation or, equivalently, the work done to perturb the system.

Additional insight into Equation 7 can be gained by further simplifying our example. To this end, we consider the case where the system has a single coupling waveguide

Please cite this article in press as: Byrnes and Foreman, Perturbing scattering resonances in non-Hermitian systems: A generalized Wigner-Smith operator formulation, Newton (2025), https://doi.org/10.1016/j.newton.2025.100194

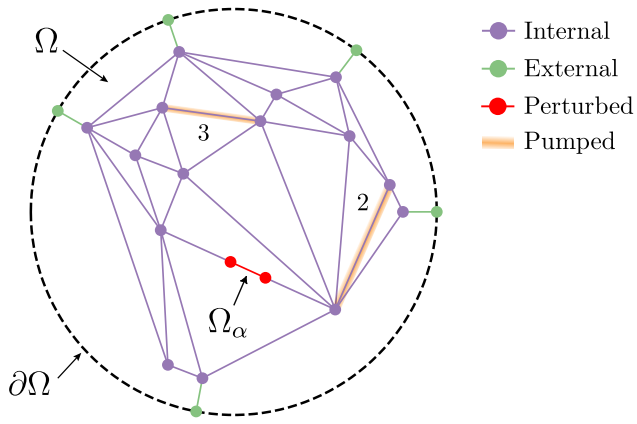

Figure 1. An example random network

Purple nodes and links are internal, while green external elements allow light to enter and exit the network. The red link (Ω_α) and highlighted links (2 and 3) correspond to those perturbed in numerical experiments described in the text.

supporting a single mode so that the scattering matrix reduces to an effective scalar reflection coefficient r_{eff}. Correspondingly, the WS operator $\mathbf{Q}_\xi$ reduces to the scalar quantity $Q_\xi = A^{-1}B_\xi$, where $A = |r_{\text{eff}}|^2$ and $B_\xi = -ir^*_{\text{eff}}\partial_\xi r_{\text{eff}}$. To evaluate these expressions at complex ω, we recast the problem into one at a real frequency but with modified material parameters. Introducing $\tilde{\epsilon} = \epsilon[1 + i\text{Im}(\omega)/\text{Re}(\omega)]$ and $\tilde{\mu} = \mu_0[1 + i\text{Im}(\omega)/\text{Re}(\omega)]$, we can show that (see methods)

$$A - 1 = \frac{\text{Re}(\omega)}{2}\int_\Omega \left[\text{Im}(\tilde{\epsilon})|\mathbf{E}|^2 + \text{Im}(\tilde{\mu})|\mathbf{H}|^2\right] dV, \quad \text{(Equation 8)}$$

where the fields should now be understood to oscillate with real frequency $\text{Re}(\omega)$. Note that the non-zero imaginary parts of $\tilde{\epsilon}$ and $\tilde{\mu}$ introduce virtual gain or loss to the system, which is an artifact of the fact that ω is actually complex. Equation 8 is an energy balance relation, as the integral on the right-hand side describes the energy dissipated (gained) within the system by the virtual loss (gain).[48] B_ω, meanwhile, is complex, with

$$\begin{aligned}\text{Re}(B_\omega) = -\frac{1}{4}\int_\Omega \Big[&\partial_{\text{Re}(\omega)}(\text{Re}(\omega)\epsilon)|\mathbf{E}|^2 + \mu_0|\mathbf{H}|^2 \\ &- 2\text{Re}(\omega)\Big(\text{Im}(\tilde{\epsilon})\text{Im}\big(\partial_{\text{Re}(\omega)}\mathbf{E}\cdot\mathbf{E}^*\big) \\ &+ \text{Im}(\tilde{\mu})\text{Im}\big(\partial_{\text{Re}(\omega)}\mathbf{H}\cdot\mathbf{H}^*\big)\Big)\Big] dV,\end{aligned} \quad \text{(Equation 9)}$$

which, up to constant factors, equals the system's stored electromagnetic energy[48] (see methods for further details). Frequency derivatives in Equation 9 are necessary to account for material dispersion. On the other hand, $\text{Im}(B_\omega) = -\partial_{\text{Re}(\omega)}A/2$ describes energy dissipation within the system. Similar expressions have been used to account for material losses in resonant systems.[49,50]

Consider now B_α and suppose that the system perturbation modifies the permittivity in a localized region $\Omega_\alpha \subset \Omega$. This might be caused by, for example, a local pressure change or a particle binding to the system. If the internal field distributions are only weakly affected by the perturbation, then $V^e_\alpha = V^m_\alpha \approx 0$ and

$$B_\alpha \approx \frac{\omega}{4}\int_\Omega \partial_\alpha\epsilon|\mathbf{E}|^2 dV. \quad \text{(Equation 10)}$$

Recalling the form of the right-hand side of Equation 6, note that the numerator will contain the factor $\Delta\alpha B_\alpha$, which, in light of Equation 10, will involve the product $\Delta\alpha\partial_\alpha\epsilon$. By assumption, outside of Ω_α, $\partial_\alpha\epsilon = 0$, while within Ω_α we have $\Delta\alpha\partial_\alpha\epsilon = \Delta\epsilon$, where $\Delta\epsilon$ is the change in ϵ. Equation 6 therefore reduces to

$$\frac{\Delta\omega_p}{\omega_p} = -\frac{1}{B_\omega}\int_{\Omega_\alpha}\Delta\epsilon|\mathbf{E}|^2 dV. \quad \text{(Equation 11)}$$

Since we have assumed high-quality-factor resonances, the virtual gain or dissipation will be weak, such that $B_\omega \approx \text{Re}(B_\omega)$, and Equation 11 is thus in full agreement with standard cavity perturbation theory.[28] It is important to stress that Equation 11 is only strictly valid for infinite-quality-factor resonances but is a reasonable approximation when the loss is weak. In contrast, Equation 3 holds more generally since no restrictions were made in its derivation. Further analysis of systems with stronger non-Hermitian effects and low-quality-factor resonances can be found in an accompanying paper.[32]

As a final remark, we note that it may be of interest to evaluate Equation 3 using experimentally measured scattering matrices. Typical experimental measurements of **S** (and thus WS operators), however, occur necessarily at real frequencies. This limitation prevents direct evaluation of the right-hand side of Equation 3 from experimental data alone. For a high-quality-factor resonance, however, the scattering matrix pole lies close to the real axis, and the resonance shift can be approximated using the right-hand side of Equation 6 measured at a real frequency close to the resonance. For resonances with low quality factors, alternative strategies are required, such as, for example, analytically continuing the scattering matrix away from the real axis from real frequency data. Techniques for rational approximations of this kind have emerged in recent years,[51] but are beyond the scope of this paper.

Numerical examples

We now turn to demonstrating the validity of our results with numerical simulations. As an example, we consider photonic networks consisting of randomly connected, single-mode dielectric waveguides, which have recently been investigated as a platform for random lasing[46,52] and in integrated photonic circuits.[53] Such systems are relatively simple to model and have non-trivial spectra. An example network, shown in Figure 1, was generated by Delaunay triangulation of a random collection of coplanar "internal" nodes (purple). An additional layer of "external" nodes (green) connect to selected internal nodes at the network periphery and serve as entry points, allowing one to define the network scattering matrix **S**. Given knowledge of the scattering properties of the

Please cite this article in press as: Byrnes and Foreman, Perturbing scattering resonances in non-Hermitian systems: A generalized Wigner-Smith operator formulation, Newton (2025), https://doi.org/10.1016/j.newton.2025.100194

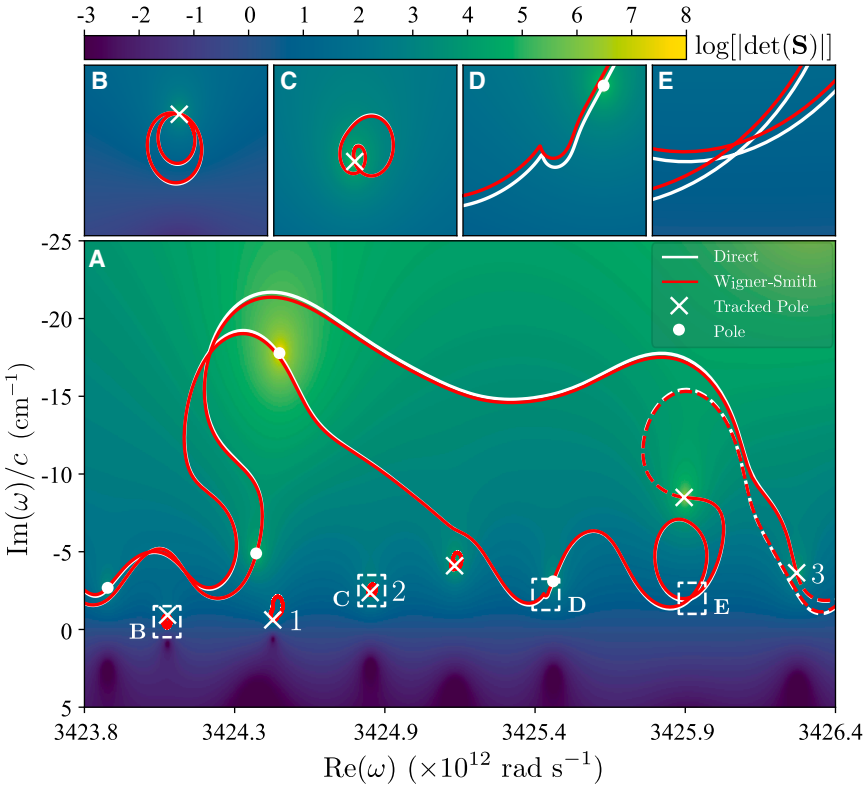

Figure 2. Perturbed pole trajectories in the complex plane

(A) Complex ω plane showing the trajectories of the network scattering matrix poles upon perturbation of Ω_α. Curves (solid for $\Delta n > 0$ and dashed $\Delta n < 0$) were traced by numerically solving $\det(\mathbf{S}^{-1}) = 0$ (white curves) and from Equation 3 (red curves). White crosses (dots) denote the (un)tracked poles. Numbered poles are those described in the numerical pumping experiment. White dashed boxes depict regions shown in (B)–(E).

network's nodes and links, **S** and its derivatives can be calculated and thus $\mathbf{Q}_\xi$ can be evaluated directly.[54] In the methods section, we demonstrate how $\mathbf{Q}_\xi$ can also be found numerically from Equation 7.

With our network, we searched for poles of **S** with frequencies $\mathrm{Re}(\omega)$ of $\sim 3,425 \times 10^{12}$ rad/s, corresponding to a vacuum wavelength of ~ 550 nm. The links were assumed to be made of glass with a refractive index n calculated using a standard Sellmeier equation.[55] Dispersion was weak in our example, and $n \approx 1.5185$ was approximately constant over the frequency range considered. The propagation of light through each link was described using exponential factors of the form $e^{\pm i\omega nL/c}$, where L is the link length. The average link length in the network was 60 μm. For simplicity, each internal node was given a randomly generated, frequency-independent scattering matrix drawn from the circular orthogonal ensemble to enforce energy conservation and reciprocity.[56] To perturb the network, we isolated a segment of a randomly chosen link (red "perturbed" segment, Ω_α, in Figure 1) and varied its refractive index n_s. Specifically, n_s was given by $n_s = n + \Delta n$, where Δn was incrementally increased from 10^{-5} to 10^{-2} in 10^4 steps (a step size of $\sim 10^{-6}$ in Δn). Note that the final value $\Delta n = 10^{-2}$ corresponded to a total phase shift in the segment $\phi = \omega \Delta n L/c$ equal to several multiples of 2π. We further introduced two virtual nodes at the ends of the perturbed segment, which were given standard Fresnel scattering matrices based on the refractive index mismatch.

Figure 2A depicts the variation of $\log[|\det(\mathbf{S})|]$ in the complex ω plane for the unperturbed network, i.e., $\Delta n = 0$. Bright regions, marked with white dots and crosses, correspond to the poles of the unperturbed network scattering matrix. Figures 2B–2E show detailed plots of the smaller regions bounded by the white dashed boxes in the main image. The positions of a subset of the poles, specifically those marked with white crosses, were tracked as Δn was increased. The trajectories followed are shown by the solid red and white lines emanating from the initial pole positions (crosses). White lines were traced by numerically solving $\det(\mathbf{S}^{-1}) = 0$ for each value of Δn. The red lines, on the other hand, were traced using Equation 3 with $\alpha = \Delta n$ to determine the pole shifts at each step (see methods for details of the calculation of $\mathbf{Q}_\alpha$). As can be seen, the WS theory agrees excellently with the direct numerical solutions. Some notable discrepancies, however, can be seen, e.g., near the top of the main image and in Figures 2D and 2E. In these regions, it was found that computed values for $\mathrm{Res}_{\omega = \omega_p} \mathrm{tr}(\mathbf{Q}_\alpha)$ were larger than for poles in other regions, implying that the poles were more sensitive to perturbations and thus moved a greater distance for each step in the simulation. For such cases, errors accrue more significantly over a large number of steps, and a smaller perturbation step size would be required to improve agreement between the different methods. Dashed red and white lines emanating from the crosses on the right-hand side of Figure 2A show the pole trajectories for $\Delta n < 0$ and show further agreement between the two methods.

Figure 2 shows several interesting features. First, note that the half-space $\mathrm{Im}(\omega) > 0$ contains dark regions for which $\det(\mathbf{S}) = 0$. These zeros can be pushed to the real axis by introducing loss to the system, whereby they correspond to coherent perfect absorption modes.[57] Note also that the poles in our data exhibit two distinct types of trajectories: some follow long, meandering paths, while others revolve around localized, closed loops. Figures 2B and 2C, in particular, demonstrate the latter type. It is important to realize that **S** is quasiperiodic in Δn since, for specific values of Δn, the additional propagation phase acquired in Ω_α will be an exact multiple of 2π. At these values, the only difference between the perturbed and unperturbed networks will

Please cite this article in press as: Byrnes and Foreman, Perturbing scattering resonances in non-Hermitian systems: A generalized Wigner-Smith operator formulation, Newton (2025), https://doi.org/10.1016/j.newton.2025.100194

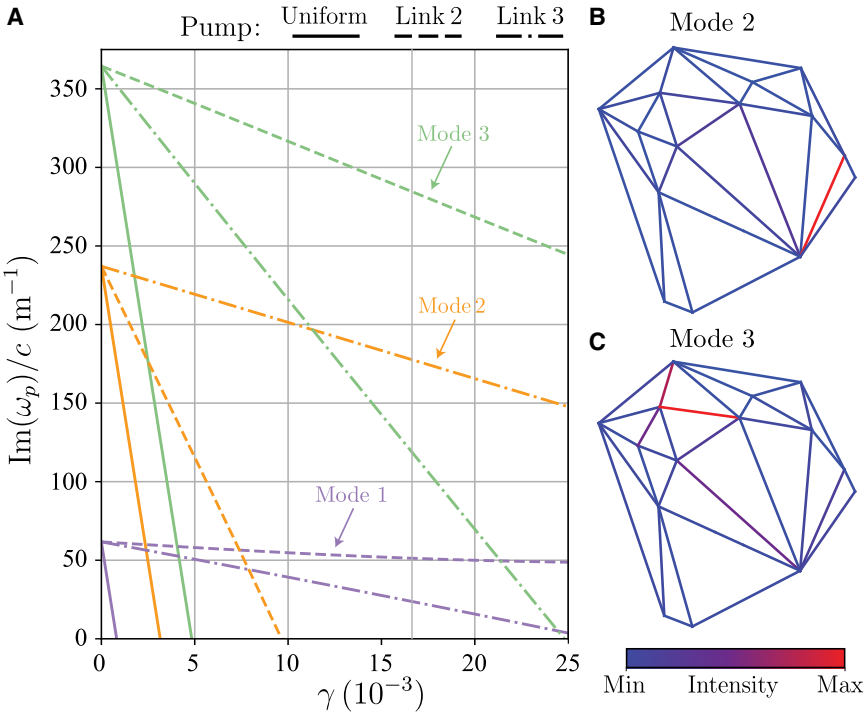

Figure 3. Selective mode pumping in a complex network

(A) Imaginary parts of selected poles as different network links are pumped (see Figure 1). Colors and line styles distinguish different modes and pumping methods respectively.

(B and C) Spatial intensity profiles of modes 2 (B) and 3 (C).

be the weak Fresnel matrices at the ends of the perturbed link segment. For the values of Δn considered, these matrices are almost perfectly transmitting and only impart weak amplitude modulations to the fields. Since the optical response of the network is dominated by interference from multiple scattering, it is significantly more sensitive to phase variations and is practically unaffected by these changes in amplitude. Poles following loop trajectories must therefore return to their original positions, while poles following open trajectories must pass through the positions of other poles of the unperturbed network (white dots in Figure 2A).

As a further application of our theory, we next considered adding gain to (or "pumping") our network, which can lead to random lasing.[52] Mathematically, gain can be introduced to the j-th link by setting its refractive index to $n_j = \mathrm{Re}(n_j) - i\gamma_j$, where $\mathrm{Re}(n_j)$ is calculated as before and $\gamma_j > 0$ is a gain coefficient taken, for simplicity, to be frequency independent over the pumping bandwidth. Adding gain causes poles to drift toward the real axis, and the pole that reaches the axis first typically determines the dominant lasing frequency.[58] Single mode lasing at arbitrary resonant frequencies is achievable by shaping the pump profile in accordance with the spatial profile of the resonant mode.[59,60] Similar selective lasing can be predicted using our theory by considering the collection of generalized WS operators associated with the gain coefficients. Specifically, for any pole ω_p and for all j, we calculate $\mathrm{Res}_{\omega=\omega_p}\mathrm{tr}(\mathbf{Q}_{\gamma_j})$, where $\mathbf{Q}_{\gamma_j}$ is the operator associated with adding gain γ_j to *only* the j-th link. In light of Equation 3, these values predict how the pole will shift when different links are pumped, thus revealing which should be pumped to optimally shift ω_p toward the threshold.

Figure 3A shows the results of the described numerical pumping experiment. The imaginary parts of three arbitrarily selected poles (distinguished by color and corresponding to the numbered poles in Figure 2A) were tracked in response to three alternate pumping methods (distinguished by line style). Solid lines track the poles when all links are pumped uniformly, in which case the narrowest resonance, mode 1 (at $3{,}424.47 \times 10^{12}$ rad/s), reaches the lasing threshold first. Alternatively, the dashed and dot-dashed lines track the poles when the links highlighted (and denoted 2 and 3, respectively) in Figure 1 were pumped in isolation. In particular, links 2 and 3 correspond to those predicted to optimally shift modes 2 (at $3{,}424.8 \times 10^{12}$ rad/s) and 3 (at $3{,}426.25 \times 10^{12}$ rad/s), respectively, toward the real axis. This predicted behavior is evident in Figure 3A, with the pumping of link 2 bringing mode 2 to the lasing threshold first (and similarly for mode/link 3). We also calculated the spatial intensity profiles of modes 2 and 3 across the network, which are shown in Figures 3B and 3C. Notably, the intensity of mode 2 (3) is strongly peaked across link 2 (3), confirming the wisdom that the optimal pump profile should conform to the mode's spatial distribution. Interestingly, however, the use of the generalized WS operator eliminated the need to explicitly calculate the mode distribution in determining the pump profile. Finally, we note that a similar strategy of selectively introducing loss to specific links could produce coherent perfect absorption of desired modes.

DISCUSSION

In this work, we have presented a novel method for calculating resonance shifts in perturbed open systems using generalized WS operators. Our work reveals the connection between generalized WS operators and resonant properties in non-Hermitian systems and further highlights their utility. Our perturbation theory is based on general complex-analytic arguments and is therefore applicable to a broad range of scenarios. Furthermore, we demonstrated that our results reduce to traditional perturbation formulas for high-quality-factor resonances. We have verified our theory numerically by tracking pole shifts caused by refractive index perturbations in a complex photonic network and in a spatially selective pumping experiment. Our work provides a novel way to analyze scattering resonances, which may be of use in cavity or nanostructure design[61] and future sensing technologies.

Please cite this article in press as: Byrnes and Foreman, Perturbing scattering resonances in non-Hermitian systems: A generalized Wigner-Smith operator formulation, Newton (2025), https://doi.org/10.1016/j.newton.2025.100194

METHODS

Derivation of the pole shift equation

In this section, we present a derivation of Equation 3, which gives the pole shift due to a system perturbation in terms of W-S operators.

As discussed in perturbation theory, it is helpful to consider the function

$$f(\omega,\alpha) = \det\left[\mathbf{S}^{-1}(\omega,\alpha)\right], \qquad \text{(Equation 12)}$$

where $\mathbf{S}$ is the scattering matrix, ω is the complex frequency, and α is a system parameter. Importantly, if ω_p is a pole of $\mathbf{S}$, then $f(\omega_p,\alpha) = 0$. We assume that all poles and zeros are of order one. Suppose that the system is perturbed so that α changes value to $\alpha' = \alpha+\Delta\alpha$, and let C be an arbitrary contour in the complex frequency plane that encircles ω_p and no other poles or zeros of $\mathbf{S}$. If $\omega \in C$, expanding f about (ω,α), we have

$$f\left(\omega_p',\alpha'\right) = f(\omega,\alpha) + \left(\omega_p' - \omega\right)\partial_\omega f(\omega,\alpha) + \Delta\alpha\partial_\alpha f(\omega,\alpha) + \cdots, \qquad \text{(Equation 13)}$$

where ω_p' is the shifted pole for the perturbed system. The higher-order terms in Equation 13 will contain factors of the form $(\omega_p' - \omega)^{n_1}\Delta\alpha^{n_2}$, where $n_1+n_2 \geq 2$. We shall neglect these terms on the grounds that the perturbation $\Delta\alpha$ and the corresponding pole shift $\Delta\omega_p$ are assumed to be small. By taking C to be sufficiently close to ω_p, we can assume that $\omega\approx\omega_p$, and thus, $\omega_p' - \omega\approx\omega_p' - \omega_p = \Delta\omega_p$. Therefore, $(\omega_p' - \omega)^{n_1}\Delta\alpha^{n_2}\approx\Delta\omega_p^{n_1}\Delta\alpha^{n_2}$ and since all terms for which $n_1+n_2 \geq 2$ are the products of multiple small quantities, we neglect them.

Since ω_p' is a resonant frequency of the perturbed system, $f(\omega_p',\alpha') = 0$. Also, since f is non-zero on C, we can divide each term in Equation 13 by $f(\omega,\alpha)$ to give (dropping functional dependencies on ω and α in our notation for clarity)

$$0 = 1 + \left(\omega_p' - \omega\right)\frac{\partial_\omega f}{f} + \Delta\alpha\frac{\partial_\alpha f}{f}. \qquad \text{(Equation 14)}$$

Letting ξ stand in place of ω and α and using standard results from matrix calculus, the logarithmic derivative of f is given by[62]

$$\frac{\partial_\xi f}{f} = \mathrm{tr}\left(\mathbf{S}\partial_\xi\mathbf{S}^{-1}\right) = -\mathrm{tr}\left(\mathbf{S}^{-1}\partial_\xi\mathbf{S}\right). \qquad \text{(Equation 15)}$$

The final equality in Equation 15 follows from the fact that

$$\partial_\xi\mathbf{S}^{-1} = -\mathbf{S}^{-1}(\partial_\xi\mathbf{S})\mathbf{S}^{-1} \qquad \text{(Equation 16)}$$

and the cyclic invariance of the trace operator.

Ideally, we would evaluate Equation 14 at $\omega = \omega_p$ and solve the resulting equation for $\Delta\omega_p$. Since f has a zero at ω_p, however, the function $\partial_\xi f/f$ has a pole at ω_p. To avoid problems associated with divergences, we proceed by calculating the residue of each term in Equation 14 at ω_p. This can be done by dividing each term by $2\pi i$ and integrating over the contour C. Clearly the unity term has zero residue. For the term containing $\partial_\alpha f/f$, it follows from Equation 15 and the definition of the W-S operator that

$$\begin{aligned}\frac{\Delta\alpha}{2\pi i}\oint_C\frac{\partial_\alpha f}{f}\mathrm{d}\omega &= -i\Delta\alpha\frac{1}{2\pi i}\oint_C\mathrm{tr}\left(-i\mathbf{S}^{-1}\partial_\alpha\mathbf{S}\right)\mathrm{d}\omega \\ &= -i\Delta\alpha\operatorname*{Res}_{\omega=\omega_p}\mathrm{tr}(\mathbf{Q}_\alpha).\end{aligned} \qquad \text{(Equation 17)}$$

The residue of the term containing $\partial_\omega f/f$ can be evaluated using the argument principle.[63] Since, by construction, f only has a single zero (at ω_p) and no poles within C, it follows that

$$\operatorname*{Res}_{\omega=\omega_p}\frac{\partial_\omega f}{f} = 1. \qquad \text{(Equation 18)}$$

Next, we make use of the fact that if the functions g and h are such that g is holomorphic at ω_p and h has a simple pole at ω_p, then

$$\operatorname*{Res}_{\omega=\omega_p} gh = g(\omega_p)\operatorname*{Res}_{\omega=\omega_p} h. \qquad \text{(Equation 19)}$$

Setting $g(\omega) = \omega_p' - \omega$ and $h = \partial_\omega f/f$, we obtain

$$\frac{1}{2\pi i}\oint_C\left(\omega_p' - \omega\right)\frac{\partial_\omega f}{f}\mathrm{d}\omega = \omega_p' - \omega_p = \Delta\omega_p. \qquad \text{(Equation 20)}$$

Having found the residue of each term in Equation 14, the resulting equation can now be solved for $\Delta\omega_p$ to give

$$\Delta\omega_p = i\Delta\alpha\operatorname*{Res}_{\omega=\omega_p}\mathrm{tr}(\mathbf{Q}_\alpha), \qquad \text{(Equation 21)}$$

which is the first equality of Equation 3.

The second equality of Equation 3 follows from the fact that

$$\operatorname*{Res}_{\omega=\omega_p}\mathrm{tr}(\mathbf{Q}_\omega) = i, \qquad \text{(Equation 22)}$$

which is a straightforward consequence of Equations 15 and 18 since

$$i = i\frac{1}{2\pi i}\oint_C\frac{\partial_\omega f}{f}\mathrm{d}\omega = \frac{1}{2\pi i}\oint_C\mathrm{tr}\left(-i\mathbf{S}^{-1}\partial_\omega\mathbf{S}\right)\mathrm{d}\omega = \operatorname*{Res}_{\omega=\omega_p}\mathrm{tr}(\mathbf{Q}_\omega). \qquad \text{(Equation 23)}$$

Finally, since $i = -1/i$, we have

$$\begin{aligned}\Delta\omega_p &= i\Delta\alpha\operatorname*{Res}_{\omega=\omega_p}\mathrm{tr}(\mathbf{Q}_\alpha) = -\Delta\alpha\frac{\mathrm{Res}_{\omega=\omega_p}\mathrm{tr}(\mathbf{Q}_\alpha)}{i} \\ &= -\Delta\alpha\frac{\mathrm{Res}_{\omega=\omega_p}\mathrm{tr}(\mathbf{Q}_\alpha)}{\mathrm{Res}_{\omega=\omega_p}\mathrm{tr}(\mathbf{Q}_\omega)},\end{aligned} \qquad \text{(Equation 24)}$$

which completes the derivation.

Please cite this article in press as: Byrnes and Foreman, Perturbing scattering resonances in non-Hermitian systems: A generalized Wigner-Smith operator formulation, Newton (2025), https://doi.org/10.1016/j.newton.2025.100194

Derivation of the volume integral form of the W-S operator

In this section, we present a derivation of Equation 7, which expresses the W-S operators in terms of volume integrals over the system.

An important observation is that the W-S operator can be factorized as $\mathbf{Q}_\xi = \mathbf{A}^{-1}\mathbf{B}_\xi$, where $\mathbf{A} = \mathbf{S}^\dagger\mathbf{S}$ and $\mathbf{B}_\xi = -i\mathbf{S}^\dagger\partial_\xi\mathbf{S}$. We proceed by deriving volume integral expressions for $\mathbf{A}$ and $\mathbf{B}_\xi$ separately and then combining the results to obtain an expression for $\mathbf{Q}_\xi$. As shall be shown, the former can be derived from a generalized Poynting theorem, while the latter can be derived from an additional energy balance relation.

Suppose that all fields are time harmonic with an implicit $e^{-i\omega t}$ dependence. The permittivity ϵ is assumed to be a real valued scalar, and the permeability μ_0 is that of free space. We begin by determining an expression for $\mathbf{A}$. Let Ω be a large surface that encapsulates the system, and let $\partial\Omega$ denote its boundary. Suppose that light is able to enter and exit the system via a finite number of waveguides that perforate $\partial\Omega$. Let $\mathbf{E}_p$ and $\mathbf{H}_p$ ($\mathbf{E}_q$ and $\mathbf{H}_q$) denote the fields throughout the system that arise due to illuminating the system by the p-th (q-th) incident field, where p (q) enumerates all of the modes in all of the waveguides. An integral version of Poynting's theorem for time harmonic fields gives[48]

$$\frac{1}{2}\int_{\partial\Omega}\left(\mathbf{E}_p\times\mathbf{H}_q^*\right)\cdot\hat{\mathbf{n}}\,dA = \frac{i}{2}\int_{\Omega}\left(\omega\mu_0\mathbf{H}_p\cdot\mathbf{H}_q^* - \omega^*\epsilon\mathbf{E}_p\cdot\mathbf{E}_q^*\right)dV, \tag{Equation 25}$$

where $\hat{\mathbf{n}}$ is an outward-pointing unit normal vector to the surface $\partial\Omega$.

Consider first the integral on the left-hand side of Equation 25, which can be written as a sum of integrals over the waveguide cross-sections. We shall assume for simplicity that these waveguides only support a single mode, but extension to multiple modes is straightforward. Around the cross-section $\partial\Omega_m$, where $\partial\Omega$ meets the m-th waveguide, we define a local Cartesian coordinate system where $\hat{\mathbf{z}}$ points out of the system along the waveguide axis and $\hat{\mathbf{x}}$ and $\hat{\mathbf{y}}$ lie within $\partial\Omega_m$, which is assumed to be at $z = 0$. Let $\mathbf{E}_{mp}$ and $\mathbf{H}_{mp}$ ($\mathbf{E}_{mq}$ and $\mathbf{H}_{mq}$) denote the fields within the m-th waveguide that arise due to illuminating the system via the p-th (q-th) waveguide. We assume that the fields within the waveguide have the forms

$$\mathbf{E}_{mp} = \delta_{mp}\mathbf{e}_m^- e^{-i\beta_m z} + S_{mp}\mathbf{e}_m^+ e^{i\beta_m z} \text{ and} \tag{Equation 26}$$

$$\mathbf{H}_{mp} = \delta_{mp}\mathbf{h}_m^- e^{-i\beta_m z} + S_{mp}\mathbf{h}_m^+ e^{i\beta_m z}, \tag{Equation 27}$$

where β_m is the waveguide propagation constant, δ_{mp} is a Kronecker delta, S_{mp} is the (m,p)-th element of the scattering matrix, and $\mathbf{e}_m^+$, $\mathbf{e}_m^-$, $\mathbf{h}_m^+$, and $\mathbf{h}_m^-$ are the vector profiles of the electric and magnetic fields, which are functions only of the transverse spatial coordinates x and y. The propagation constant can be expressed as $\beta_m = n_m^{\text{eff}}k_0$, where $n_m^{\text{eff}} = \sqrt{\epsilon_m^{\text{eff}}/\epsilon_0}$ is an effective refractive index and $k_0 = \omega/c$ is the vacuum wavenumber, where c is the speed of light in vacuum. Using Equations 26 and 27, we have

$$\begin{aligned}\frac{1}{2}&\int_{\partial\Omega_m}\left(\mathbf{E}_{mp}\times\mathbf{H}_{mq}^*\right)\cdot\hat{\mathbf{n}}\,dA\\ &= \frac{1}{2}\int_{\partial\Omega_m}\left[\left(\delta_{mp}\mathbf{e}_{m,t}^- + S_{mp}\mathbf{e}_{m,t}^+\right)\times\left(\delta_{mq}\mathbf{h}_{m,t}^{-*} + S_{mq}^*\mathbf{h}_{m,t}^{+*}\right)\right]\cdot\hat{\mathbf{z}}\,dA\\ &= \frac{1}{2}\left(\delta_{mp}\delta_{mq} - \delta_{mp}S_{mq}^* + \delta_{mq}S_{mp} - S_{mp}S_{mq}^*\right)\\ &\quad\int_{\partial\Omega_m}\left(\mathbf{e}_{m,t}\times\mathbf{h}_{m,t}^*\right)\cdot\hat{\mathbf{z}}\,dA,\end{aligned} \tag{Equation 28}$$

where $\mathbf{e}_{m,t}^\pm$ and $\mathbf{h}_{m,t}^\pm$ are the transverse parts of $\mathbf{e}_m^\pm$ and $\mathbf{h}_m^\pm$. Note that we have adopted the convention in which $\mathbf{e}_{m,t} = \mathbf{e}_{m,t}^- = \mathbf{e}_{m,t}^+$ and $\mathbf{h}_{m,t} = \mathbf{h}_{m,t}^- = -\mathbf{h}_{m,t}^+$, which can be done without loss of generality.[64]

The integral on the right side of the final equality of Equation 28 warrants some discussion. Ideally, we would assert that the integral is equal to unity by some appropriate mode normalization. For materials with loss or gain, however, this cannot be assumed to be the case. In our case, even though ϵ is real, we are still faced with virtual loss or gain in virtue of the fact that ω is complex (see physical interpretation of complex frequency and derivation of energy interpretation of W-S operators). Since, however, we are only concerned with high-quality-factor resonances for which $\text{Im}(\omega)/\text{Re}(\omega) \ll 1$, this effect is weak, and we are permitted to treat $\mathbf{e}_{m,t}$ and $\mathbf{h}_{m,t}$ as though the waveguides were lossless, allowing us to assert[64]

$$\frac{1}{2}\int_{\partial\Omega_m}\left(\mathbf{e}_{m,t}\times\mathbf{h}_{m,t}^*\right)\cdot\hat{\mathbf{z}}\,dA = 1. \tag{Equation 29}$$

If the external waveguides supported multiple modes, we would also be permitted to assume mode orthogonality in the sense that the integral in Equation 29 would vanish if $\mathbf{e}_t$ and $\mathbf{h}_t$ were associated with two different modes.

Armed with Equation 29, summing Equation 28 over m gives the integral over all of $\partial\Omega$, which is given by

$$\frac{1}{2}\int_{\partial\Omega}\left(\mathbf{E}_p\times\mathbf{H}_q^*\right)\cdot\hat{\mathbf{n}}\,dA = \left(\mathbf{I} - \mathbf{S}^\dagger\mathbf{S} + \mathbf{S} - \mathbf{S}^\dagger\right)_{qp}, \tag{Equation 30}$$

where $\mathbf{I}$ is the identity matrix and the subscript qp indicates that we are looking at the (q, p)-th element of the matrix expression within the parentheses. In order to ease notation, let

$$U_{qp}^e = \frac{1}{4}\mathbf{E}_p\cdot\mathbf{E}_q^* \text{ and} \tag{Equation 31}$$

$$U^m_{qp} = \frac{1}{4}\mathbf{H}_p\cdot\mathbf{H}^*_q, \quad \text{(Equation 32)}$$

and let $\mathbf{U}^e$ and $\mathbf{U}^m$ denote the matrices whose (q,p)-th elements are U^e_{qp} and U^m_{qp}, respectively. Equation 25 can then be written as the matrix equation

$$\mathbf{I} - \mathbf{S}^\dagger\mathbf{S} + \mathbf{S} - \mathbf{S}^\dagger = 2i\int_\Omega (\omega\mu_0\mathbf{U}^m - \omega^*\epsilon\mathbf{U}^e)\,dV. \quad \text{(Equation 33)}$$

In order to extract $\mathbf{S}^\dagger\mathbf{S}$ from Equation 33, we take the Hermitian part of both sides. The Hermitian and skew Hermitian parts of a matrix $\mathbf{M}$, which we denote as $\mathrm{Her}(\mathbf{M})$ and $\mathrm{SHer}(\mathbf{M})$, respectively, are defined by

$$\mathrm{Her}(\mathbf{M}) = \frac{\mathbf{M}+\mathbf{M}^\dagger}{2} \text{ and} \quad \text{(Equation 34)}$$

$$\mathrm{SHer}(\mathbf{M}) = \frac{\mathbf{M} - \mathbf{M}^\dagger}{2}. \quad \text{(Equation 35)}$$

Taking the Hermitian part eliminates the skew Hermitian matrix $\mathbf{S} - \mathbf{S}^\dagger$ from the left side of Equation 33, leaving only the Hermitian matrix $\mathbf{I} - \mathbf{S}^\dagger\mathbf{S}$. Finally, we find $\mathbf{A}$ to be

$$\mathbf{A} = \mathbf{S}^\dagger\mathbf{S} = \mathbf{I} + 2\mathrm{Im}(\omega)\int_\Omega (\epsilon\mathbf{U}^e + \mu_0\mathbf{U}^m)\,dV. \quad \text{(Equation 36)}$$

Note that if $\mathrm{Im}(\omega) = 0$, the system is truly lossless, and the integral in Equation 36 vanishes, recovering the usual unitarity relation for $\mathbf{S}$.

We now turn to the problem of determining an integral equation for $\mathbf{B}_\xi$. For our starting point, it can be shown in general that, on the basis of energy conservation (see, for example, Geyi[48]),

$$\frac{i}{4}\int_{\partial\Omega}\left(\mathbf{E}_p\times\partial_\xi\mathbf{H}^*_q \pm \partial_\xi\mathbf{E}_p\times\mathbf{H}^*_q\right)\cdot\hat{\mathbf{n}}\,dA = \int_\Omega\Big[\partial_\xi(\omega^*\epsilon)U^e_{qp} \mp \partial_\xi\omega\mu_0 U^m_{qp} + \omega^*\epsilon\left(V^{e*}_{\xi,pq} \pm V^e_{\xi,qp}\right) - \omega\mu_0\left(V^{m*}_{\xi,pq} \pm V^m_{\xi,qp}\right)\Big]\,dV, \quad \text{(Equation 37)}$$

where we define

$$V^e_{\xi,qp} = \frac{1}{4}\partial_\xi\mathbf{E}_p\cdot\mathbf{E}^*_q \text{ and} \quad \text{(Equation 38)}$$

$$V^m_{\xi,qp} = \frac{1}{4}\partial_\xi\mathbf{H}_p\cdot\mathbf{H}^*_q. \quad \text{(Equation 39)}$$

Note that Equation 37 is, in fact, a pair of equations, as one may choose either the upper or lower set of plus and minus signs. The surface integral on the left-hand side of Equation 37 can be evaluated using similar steps to those in deriving Equation 28, taking appropriate derivatives and conjugates of Equations 26 and 27 as required. For the m-th waveguide, we find

$$\frac{1}{4}\int_{\partial\Omega_m}\left(\mathbf{E}_{mp}\times\partial_\xi\mathbf{H}^*_{mq} \pm \partial_\xi\mathbf{E}_{mp}\times\mathbf{H}^*_{mq}\right)\cdot\hat{\mathbf{z}}\,dA = \frac{1}{2}\left(-\delta_{mp}\partial_\xi S^*_{mq} - S_{mp}\partial_\xi S^*_{mq} \pm \delta_{mq}\partial_\xi S_{mp} \mp S^*_{mq}\partial_\xi S_{mp}\right) + \frac{1}{2}\left(\delta_{mp}\delta_{mq} - \delta_{mp}S^*_{mq} + \delta_{mq}S_{mp} - S_{mp}S^*_{mq}\right) \int_{\partial\Omega_m}\left(\mathbf{e}_{m,t}\times\partial_\xi\mathbf{h}^*_{m,t} \pm \partial_\xi\mathbf{e}_{m,t}\times\mathbf{h}^*_{m,t}\right)\cdot\hat{\mathbf{z}}\,dA. \quad \text{(Equation 40)}$$

Assuming that the transverse mode profiles $\mathbf{e}_{m,t}$ and $\mathbf{h}_{m,t}$ only weakly depend on ξ, the integral in the final term of Equation 40 vanishes. Summing the resulting equation over m gives

$$\frac{i}{4}\int_{\partial\Omega}\left(\mathbf{E}_p\times\partial_\xi\mathbf{H}^*_q \pm \left(\partial_\xi\mathbf{E}_p\right)\times\mathbf{H}^*_q\right)\cdot\hat{\mathbf{n}}\,dA = \frac{1}{2}[-i\partial_\xi\mathbf{S}^\dagger - i\partial_\xi\mathbf{S}^\dagger\mathbf{S} \pm i\partial_\xi\mathbf{S} \mp i\mathbf{S}^\dagger\partial_\xi\mathbf{S}]_{qp} \quad \text{(Equation 41)}$$

and, as before, Equation 37 can therefore be written as the matrix equation

$$\frac{1}{2}\left(-i\partial_\xi\mathbf{S}^\dagger - i\partial_\xi\mathbf{S}^\dagger\mathbf{S} \pm i\partial_\xi\mathbf{S} \mp i\mathbf{S}^\dagger\partial_\xi\mathbf{S}\right) = \int_\Omega\left[\partial_\xi(\omega^*\epsilon)\mathbf{U}^e \mp \partial_\xi\omega\mu_0\mathbf{U}^m + \omega^*\epsilon\left(\mathbf{V}^{e\dagger}_\xi \pm \mathbf{V}^e_\xi\right) - \omega\mu_0\left(\mathbf{V}^{m\dagger}_\xi \pm \mathbf{V}^m_\xi\right)\right]dV, \quad \text{(Equation 42)}$$

where $\mathbf{V}^e_\xi$ ($\mathbf{V}^m_\xi$) is the matrix whose (q,p)-th element is $V^e_{\xi,qp}$ ($V^m_{\xi,qp}$). To isolate $-i\mathbf{S}^\dagger\partial_\xi\mathbf{S}$, we take the skew Hermitian parts of both sides of Equation 42 with the upper set of plus and minus signs and the Hermitian parts of both sides of Equation 42 with the lower set of plus and minus signs. This gives the pair of equations

$$\mathrm{SHer}\left(-i\mathbf{S}^\dagger\partial_\xi\mathbf{S}\right) = -i\int_\Omega\left[\partial_\xi(\mathrm{Im}(\omega)\epsilon)\mathbf{U}^e + \partial_\xi\mathrm{Im}(\omega)\mu_0\mathbf{U}^m - 2i\mathrm{Im}(\omega)\left(\epsilon\mathrm{Her}\left(\mathbf{V}^e_\xi\right) + \mu_0\mathrm{Her}\left(\mathbf{V}^m_\xi\right)\right)\right]dV \text{ and} \quad \text{(Equation 43)}$$

$$\mathrm{Her}\left(-i\mathbf{S}^\dagger\partial_\xi\mathbf{S}\right) = -\int_\Omega\left[\partial_\xi(\mathrm{Re}(\omega)\epsilon)\mathbf{U}^e + \partial_\xi\mathrm{Re}(\omega)\mu_0\mathbf{U}^m - 2i\mathrm{Im}(\omega)\left(\epsilon\mathrm{SHer}\left(\mathbf{V}^e_\xi\right) + \mu_0\mathrm{SHer}\left(\mathbf{V}^m_\xi\right)\right)\right]dV. \quad \text{(Equation 44)}$$

Next, since, by definition,

$$\mathbf{B}_\xi = -i\mathbf{S}^\dagger\partial_\xi\mathbf{S} = \mathrm{Her}(-i\mathbf{S}\partial_\xi\mathbf{S}) + \mathrm{SHer}(-i\mathbf{S}^\dagger\partial_\xi\mathbf{S}), \quad \text{(Equation 45)}$$

Please cite this article in press as: Byrnes and Foreman, Perturbing scattering resonances in non-Hermitian systems: A generalized Wigner-Smith operator formulation, Newton (2025), https://doi.org/10.1016/j.newton.2025.100194

Equations 43 and 44 can be combined to give

$$\mathbf{B}_\xi = -\int_\Omega \left[\partial_\xi(\omega\epsilon)\mathbf{U}^e + \partial_\xi\omega\mu_0\mathbf{U}^m + 2i\mathrm{Im}(\omega)\left(\epsilon\mathbf{V}_\xi^e + \mu_0\mathbf{V}_\xi^m\right)\right] dV. \quad \text{(Equation 46)}$$

Finally, combining $\mathbf{A}$ and $\mathbf{B}_\xi$, we arrive at

$$\mathbf{Q}_\xi = \left(\mathbf{I} + 2\mathrm{Im}(\omega)\int_\Omega (\epsilon\mathbf{U}^e + \mu_0\mathbf{U}^m)\, dV\right)^{-1} \left(-\int_\Omega \left[\partial_\xi(\omega\epsilon)\mathbf{U}^e + \partial_\xi\omega\mu_0\mathbf{U}^m + 2i\mathrm{Im}(\omega)\left(\epsilon\mathbf{V}_\xi^e + \mu_0\mathbf{V}_\xi^m\right)\right] dV\right), \quad \text{(Equation 47)}$$

which is Equation 7.

Physical interpretation of complex frequency and derivation of energy interpretation of W-S operators

In this section, we discuss the physical interpretation of complex frequencies and derive Equations 8 and 9.

Since $\omega = \mathrm{Re}(\omega)[1 + i\mathrm{Im}(\omega)/\mathrm{Re}(\omega)]$, Maxwell's curl equations throughout the system can be written as

$$\nabla\times\mathbf{E} = i\omega\mu_0\mathbf{H} = i\mathrm{Re}(\omega)\tilde{\mu}\mathbf{H} \text{ and} \quad \text{(Equation 48)}$$

$$\nabla\times\mathbf{H} = -i\omega\epsilon\mathbf{E} = -i\mathrm{Re}(\omega)\tilde{\epsilon}\mathbf{E}, \quad \text{(Equation 49)}$$

where $\tilde{\epsilon} = \epsilon[1 + i\mathrm{Im}(\omega)/\mathrm{Re}(\omega)]$ and $\tilde{\mu} = \mu_0[1 + i\mathrm{Im}(\omega)/\mathrm{Re}(\omega)]$. This demonstrates a physical equivalence between two different points of view. On the one hand, we may think of the system as having *real* material parameters ϵ and μ_0 but supporting waves at a *complex* frequency ω. On the other hand, we may instead imagine that the waves oscillate at the *real* frequency $\mathrm{Re}(\omega)$ but in a system with *complex* material parameters $\tilde{\epsilon}$ and $\tilde{\mu}$. Since Maxwell's equations are the same in either case, the two viewpoints are physically equivalent. The latter, however, is perhaps more familiar, and the imaginary parts of the permittivity and permeability are well understood as representing loss or gain. A wave possessing a complex frequency therefore also exhibits loss or gain, depending on the sign of $\mathrm{Im}(\omega)$.

Using the definitions of $\tilde{\epsilon}$ and $\tilde{\mu}$ in Equation 36, it is straightforward to show that

$$\mathbf{A} = \mathbf{I} + 2\mathrm{Re}(\omega)\int_\Omega [\mathrm{Im}(\tilde{\epsilon})\mathbf{U}^e + \mathrm{Im}(\tilde{\mu})\mathbf{U}^m]\, dV, \quad \text{(Equation 50)}$$

which, when restricted to the single mode example discussed in connection to electromagnetic theory, which enforces the transformations $\mathbf{I}\to 1$, $\mathbf{U}^e\to\frac{1}{4}|\mathbf{E}|^2$, and $\mathbf{U}^m\to\frac{1}{4}|\mathbf{H}|^2$, reduces to Equation 8. Similarly, in terms of $\tilde{\epsilon}$ and $\tilde{\mu}$, Equation 46 becomes

$$\mathbf{B}_\xi = -\int_\Omega \left[\partial_\xi(\mathrm{Re}(\omega)\tilde{\epsilon})\mathbf{U}^e + \partial_\xi(\mathrm{Re}(\omega)\tilde{\mu})\mathbf{U}^m + 2i\mathrm{Re}(\omega)\left(\mathrm{Im}(\tilde{\epsilon})\mathbf{V}_\xi^e + \mathrm{Im}(\tilde{\mu})\mathbf{V}_\xi^m\right)\right] dV. \quad \text{(Equation 51)}$$

Restricting again to a single mode, where now $\mathbf{V}_\xi^e\to\frac{1}{4}\partial_\xi\mathbf{E}\cdot\mathbf{E}^*$ and $\mathbf{V}_\xi^m\to\frac{1}{4}\partial_\xi\mathbf{H}\cdot\mathbf{H}^*$, and taking the real part of Equation 51, we find

$$\mathrm{Re}(B_\xi) = -\frac{1}{4}\int_\Omega \left[\partial_\xi(\mathrm{Re}(\omega)\varepsilon)|\mathbf{E}|^2 + \partial_\xi\mathrm{Re}(\omega)\mu_0|\mathbf{H}|^2 - 2\mathrm{Re}(\omega)(\mathrm{Im}(\tilde{\varepsilon})\mathrm{Im}(\partial_\xi\mathbf{E}\cdot\mathbf{E}^*) + \mathrm{Im}(\tilde{\mu})\mathrm{Im}(\partial_\xi\mathbf{H}\cdot\mathbf{H}^*))\right] dV. \quad \text{(Equation 52)}$$

Next, note that for any holomorphic function f of a complex variable z, we have $\partial_z f = \partial_{\mathrm{Re}(z)} f$.[63] Assuming that all functions in Equation 52 that need to be differentiated are complex differentiable with respect to ω, we can set $\xi = \omega$ in Equation 52 and make the substitution $\partial_\omega\to\partial_{\mathrm{Re}(\omega)}$ to obtain

$$\mathrm{Re}(B_\omega) = -\frac{1}{4}\int_\Omega \left[\partial_{\mathrm{Re}(\omega)}(\mathrm{Re}(\omega)\varepsilon)|\mathbf{E}|^2 + \mu_0|\mathbf{H}|^2 - 2\mathrm{Re}(\omega)\left(\mathrm{Im}(\tilde{\varepsilon})\mathrm{Im}(\partial_{\mathrm{Re}(\omega)}\mathbf{E}\cdot\mathbf{E}^*)\right) + \mathrm{Im}(\tilde{\mu})\mathrm{Im}\left(\partial_{\mathrm{Re}(\omega)}\mathbf{H}\cdot\mathbf{H}^*\right)\right] dV, \quad \text{(Equation 53)}$$

which is Equation 9. Finally, taking the imaginary part of Equation 51 for $\xi = \omega$ gives

$$\mathrm{Im}(B_\omega) = -\frac{1}{4}\int_\Omega \left[\partial_{\mathrm{Re}(\omega)}(\mathrm{Re}(\omega)\mathrm{Im}(\tilde{\varepsilon}))|\mathbf{E}|^2 + \partial_{\mathrm{Re}(\omega)}(\mathrm{Re}(\omega)\mathrm{Im}(\tilde{\mu}))|\mathbf{H}|^2 + 2\mathrm{Re}(\omega)\left(\mathrm{Im}(\tilde{\varepsilon})\mathrm{Re}(\partial_{\mathrm{Re}(\omega)}\mathbf{E}\cdot\mathbf{E}^*)\right) + \mathrm{Im}(\tilde{\mu})\mathrm{Re}\left(\partial_{\mathrm{Re}(\omega)}\mathbf{H}\cdot\mathbf{H}^*\right)\right] dV. \quad \text{(Equation 54)}$$

Since

$$\mathrm{Re}(\partial_\omega\mathbf{E}\cdot\mathbf{E}^*) = \frac{1}{2}(\partial_\omega\mathbf{E}\cdot\mathbf{E}^* + \partial_\omega\mathbf{E}^*\cdot\mathbf{E}) = \frac{1}{2}\partial_\omega|\mathbf{E}|^2 \quad \text{(Equation 55)}$$

and, similarly, $\mathrm{Re}(\partial_\omega\mathbf{H}\cdot\mathbf{H}^*) = \frac{1}{2}\partial_\omega|\mathbf{H}|^2$, Equation 54 can be simplified to give

$$\mathrm{Im}(B_\omega) = -\frac{1}{2}\partial_{\mathrm{Re}(\omega)}\left(\frac{\mathrm{Re}(\omega)}{2}\int_\Omega \left[\mathrm{Im}(\tilde{\varepsilon})|\mathbf{E}|^2 + \mathrm{Im}(\tilde{\mu})|\mathbf{H}|^2\right] dV\right) = -\frac{1}{2}\partial_{\mathrm{Re}(\omega)}A, \quad \text{(Equation 56)}$$

which shows that $\mathrm{Im}(B_\omega)$ is related to energy dissipation within the system.

Please cite this article in press as: Byrnes and Foreman, Perturbing scattering resonances in non-Hermitian systems: A generalized Wigner-Smith operator formulation, Newton (2025), https://doi.org/10.1016/j.newton.2025.100194

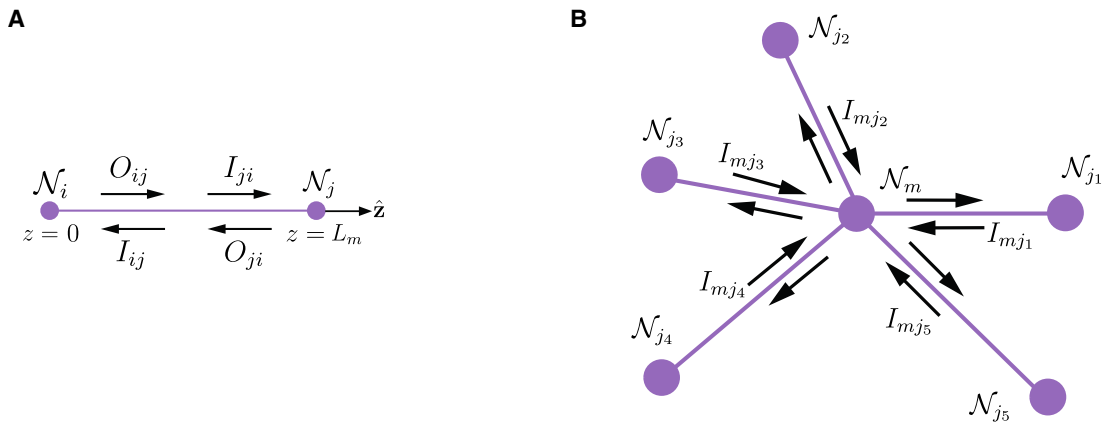

Figure 4. Geometry of network components

(A) Link connecting node $\mathcal{N}_i$ and node $\mathcal{N}_j$. I_{ij} and I_{ji} (O_{ij} and O_{ji}) denote complex amplitudes of waves entering (leaving) $\mathcal{N}_i$ at $z = 0$ and $\mathcal{N}_j$ at $z = L_m$, respectively.

(B) Node $\mathcal{N}_m$ connected to multiple adjoining nodes $\mathcal{N}_{j_1}, \cdots, \mathcal{N}_{j_5}$. $I_{mj_1}, \cdots, I_{mj_5}$ denote complex amplitudes of waves entering $\mathcal{N}_m$ from the adjoining nodes.

Evaluation of the W-S volume integrals for complex photonic networks

In this section, we show how to evaluate the volume integrals appearing in Equation 47 for a complex photonic network. The structure and properties of these networks are discussed in numerical examples.

The first integral in Equation 47 is

$$\mathbf{A} - \mathbf{I} = 2\mathrm{Im}(\omega)\int_{\Omega}(\epsilon\mathbf{U}^e + \mu_0\mathbf{U}^m)\,\mathrm{d}V. \qquad \text{(Equation 57)}$$

Integrating over Ω requires integrating over all of the N_{node} nodes and N_{link} links in the network as well as the fields in the surrounding space. We can decompose Ω into a union of subsets

$$\Omega = \Omega^{\text{space}} \cup \Omega^{\text{link}} \cup \Omega^{\text{node}} = \Omega^{\text{space}} \cup \left(\Omega_1^{\text{link}} \cup \ldots \cup \Omega_{N_{\text{link}}}^{\text{link}}\right) \cup \left(\Omega_1^{\text{node}} \cup \ldots \cup \Omega_{N_{\text{node}}}^{\text{node}}\right), \qquad \text{(Equation 58)}$$

where Ω_m^{link} is the volume occupied by the m-th link, Ω_m^{node} is the volume occupied by the m-th node, and Ω^{space} is the volume occupied by the remaining space around the links and nodes. Assuming the system does not support leaky modes, the fields in the space around the links and nodes will be evanescent, decaying away from the network components. If necessary, we may expand the volumes Ω_m^{link} and Ω_m^{node} beyond the physical extent of the network components so as to contain these evanescent fields up to a point where they have sufficiently decayed and no longer significantly contribute to the integrals. The integral over the remaining space Ω^{space} can then be be neglected.

Consider evaluating the integral in Equation 57 over Ω_m^{link} and suppose that this link connects the i-th and j-th nodes $\mathcal{N}_i$ and $\mathcal{N}_j$. A diagram of the link is given in Figure 4A. We define a local Cartesian coordinate system for the link, similar to that used in derivation of the volume integral form of the W-S operator. The unit vector $\hat{\mathbf{z}}$ is assumed to be parallel to the link's axis and points into the link from $\mathcal{N}_i$ at $z = 0$. The link extends to $z = L_m$, where it meets $\mathcal{N}_j$, such that L_m is the length of the link. To keep our calculations relatively simple, we assume that each link is weakly guiding with an effective refractive index $n_m^{\text{eff}} = c\sqrt{\epsilon_m^{\text{eff}}\mu_0}$, uniform in the z direction, and approximately constant over transverse cross-sections. We also assume that each link supports a single mode, which, given the weak guiding assumption, has negligible z component and transverse fields that satisfy[64]

$$\mathbf{h}_{m,t} = Y_m^{\text{eff}}\hat{\mathbf{z}} \times \mathbf{e}_{m,t}, \qquad \text{(Equation 59)}$$

where $Y_m^{\text{eff}} = \sqrt{\epsilon_m^{\text{eff}}/\mu_0}$ is the link's admittance. We can now derive individual normalization equations for $\mathbf{e}_{m,t}$ and $\mathbf{h}_{m,t}$. Let $\partial\Omega_m^{\text{link}}$ be a transverse cross-section of the link (for any value of z). Recalling Equation 29, we have

$$1 = \frac{1}{2}\int_{\partial\Omega_m^{\text{link}}}\left(\mathbf{e}_{m,t} \times \mathbf{h}_{m,t}^*\right)\cdot\hat{\mathbf{z}}\,\mathrm{d}A = \frac{Y_m^{\text{eff}}}{2}\int_{\partial\Omega_m^{\text{link}}}\left[\mathbf{e}_{m,t} \times \left(\hat{\mathbf{z}} \times \mathbf{e}_{m,t}^*\right)\right]\cdot\hat{\mathbf{z}}\,\mathrm{d}A = \frac{Y_m^{\text{eff}}}{2}\int_{\partial\Omega_m^{\text{link}}}\mathbf{e}_{m,t}\cdot\mathbf{e}_{m,t}^*\,\mathrm{d}A, \qquad \text{(Equation 60)}$$

from which it follows that

$$\frac{1}{2}\int_{\partial\Omega_m^{\text{link}}}\mathbf{e}_{m,t}\cdot\mathbf{e}_{m,t}^*\,\mathrm{d}A = \frac{1}{Y_m^{\text{eff}}}. \qquad \text{(Equation 61)}$$

Similarly,

$$\frac{1}{2}\int_{\partial\Omega_m^{\text{link}}}\mathbf{h}_{m,t}\cdot\mathbf{h}_{m,t}^*\,\mathrm{d}A = \frac{\left(Y_m^{\text{eff}}\right)^2}{2}\int_{\partial\Omega_m^{\text{link}}}\left(\hat{\mathbf{z}} \times \mathbf{e}_{m,t}\right)\cdot\left(\hat{\mathbf{z}} \times \mathbf{e}_{m,t}^*\right)\mathrm{d}A = \frac{\left(Y_m^{\text{eff}}\right)^2}{2}\int_{\partial\Omega_m^{\text{link}}}\mathbf{e}_{m,t}\cdot\mathbf{e}_{m,t}^*\,\mathrm{d}A = Y_m^{\text{eff}}. \qquad \text{(Equation 62)}$$

Please cite this article in press as: Byrnes and Foreman, Perturbing scattering resonances in non-Hermitian systems: A generalized Wigner-Smith operator formulation, Newton (2025), https://doi.org/10.1016/j.newton.2025.100194

The fields within the link that arise due to illuminating the system through the p-th external link are given by

$$\mathbf{E}_{mp} = \left(O_{ij,p}e^{i\beta_m z} + I_{ij,p}e^{-i\beta_m z}\right)\mathbf{e}_{m,t} \text{ and} \quad \text{(Equation 63)}$$

$$\mathbf{H}_{mp} = \left(O_{ij,p}e^{i\beta_m z} - I_{ij,p}e^{-i\beta_m z}\right)\mathbf{h}_{m,t}, \quad \text{(Equation 64)}$$

where $O_{ij,p}$ denotes the field amplitude that enters the link at $z = 0$ from $\mathcal{N}_i$ and propagates toward $\mathcal{N}_j$ and $I_{ij,p}$ is the field amplitude that exits the link at $z = 0$, entering $\mathcal{N}_i$, having arrived from $\mathcal{N}_j$. Note that the link index m defines the pair of indices ij uniquely. Integrating the field products over Ω^{link} amounts to employing the normalization conditions in Equations 61 and 62 to handle the transverse coordinates and integrating the exponential functions with respect to z. Summing the results over m, we ultimately arrive at

$$2\text{Im}(\omega)\int_{\Omega^{\text{link}}}\left(\varepsilon U^e_{qp} + \mu_0 U^m_{qp}\right)\,\text{d}V = \sum_m \Big[O_{ij,p}O^*_{ij,q}\left(e^{-2\text{Im}(\omega)n_m^{\text{eff}}L_m/c_0} - 1\right) + I_{ij,p}I^*_{ij,q}\left(1 - e^{2\text{Im}(\omega)n_m^{\text{eff}}L_m/c_0}\right)\Big], \quad \text{(Equation 65)}$$

which expresses the integral in terms of the internal field components.

Consider next evaluating the integral in Equation 57 over Ω^{node}_m. Suppose that the m-th node $\mathcal{N}_m$ is connected to a collection of other nodes $\mathcal{N}_{j_1}, \mathcal{N}_{j_2}, \ldots$ with indices $j_1, j_2, \ldots$ by a collection of links. The geometry of the node is depicted in Figure 4B. In general, evaluating the integral requires a model for the fields within the node. For simplicity, we shall instead evaluate the integral indirectly. Recall that the integral in question originated from Equation 36, which was derived from a generalized Poynting theorem over the extent of the network. We can instead apply Poynting's theorem to Ω^{node}_m to obtain a similar equation to Equation 36 for the node integral in terms of the node scattering matrix $\mathbf{S}_m$. Unlike in our derivation of Equation 36, however, we cannot use Equations 26 and 27 for the fields but must instead use expressions for the internal network fields, similar to those in Equations 63 and 64. Repeating the derivation of Equation 36 with the correct field expressions, we obtain

$$2\text{Im}(\omega)\int_{\Omega^{\text{node}}_m}\left(\epsilon U^e_{qp} + \mu_0 U^m_{qp}\right)\,\text{d}V = \mathbf{i}^\dagger_{mq}\left(\mathbf{S}^\dagger_m\mathbf{S}_m - \mathbf{I}\right)\mathbf{i}_{mp}, \quad \text{(Equation 66)}$$

where $\mathbf{i}_{mp} = (I_{mj_1,p}, I_{mj_2,p}, \ldots)^{\text{T}}$ is a vector containing components of all of the fields that are incident upon the node when the network is illuminated via the p-th mode. $\mathbf{i}_{mq} = (I_{mj_1,q}, I_{mj_2,q}, \ldots)^{\text{T}}$ is defined similarly. Summing the result of Equation 66 over m gives the total integral over Ω^{node}.

Consider now the second integral that appears in Equation 47, i.e.,

$$\mathbf{B}_\xi = -\int_\Omega \left[\partial_\xi(\omega\epsilon)\mathbf{U}^e + \partial_\xi\omega\mu_0\mathbf{U}^m + 2i\text{Im}(\omega)\left(\epsilon\mathbf{V}^e_\xi + \mu_0\mathbf{V}^m_\xi\right)\right]\text{d}V. \quad \text{(Equation 67)}$$

As before, we can assume that the integral over Ω^{space} is negligible. Evaluating the integral over the network's links can be done using analogous steps to those used in deriving Equation 65. The algebra is somewhat lengthy, and there is little additional insight to be gained from a detailed presentation. The final result is

$$-\int_{\Omega^{\text{link}}}\left[\partial_\xi(\omega\varepsilon)U^e_{qp} + \partial_\xi\omega\mu_0 U^m_{qp} + 2i\text{Im}(\omega)\left(\varepsilon V^e_{\xi,qp} + \mu_0 V^m_{\xi,qp}\right)\right]\text{d}V = \sum_m\Bigg(\partial_\xi\left(n_m^{\text{eff}}k_0\right)L_m\Big(O_{ij,p}O^*_{ij,q}e^{-2\text{Im}(\omega)n_m^{\text{eff}}L_m/c_0} + I_{ij,p}I^*_{ij,q}e^{2\text{Im}(\omega)n_m^{\text{eff}}L_m/c_0}\Big) + \frac{\text{Im}(\omega)}{2\text{Re}(\omega)}\frac{\partial_\xi n_m^{\text{eff}}}{n_m^{\text{eff}}}\Big[O_{ij,p}I^*_{ij,q}\left(e^{2i\text{Re}(\omega)n_m^{\text{eff}}L_m/c_0} - 1\right) + I_{ij,p}O^*_{ij,q}\left(1 - e^{-2i\text{Re}(\omega)n_m^{\text{eff}}L_m/c_0}\right)\Big] + i\Big[\partial_\xi O_{ij,p}O^*_{ij,q}\left(1 - e^{-2\text{Im}(\omega)n_m^{\text{eff}}L_m/c_0}\right) + \partial_\xi I_{ij,p}I^*_{ij,q}\left(e^{2\text{Im}(\omega)n_m^{\text{eff}}L_m/c_0} - 1\right)\Big]\Bigg). \quad \text{(Equation 68)}$$

Evaluating the integral over the network's nodes can also be done indirectly by repeating the derivation of Equation 46 but over Ω^{node}_m using the internal fields at the node boundary. This time, we obtain

$$-\int_{\Omega^{\text{node}}_m}\left[\partial_\xi(\omega\varepsilon)U^e_{qp} + \partial_\xi\omega\mu_0 U^m_{qp} + 2i\text{Im}(\omega)\left(\varepsilon V^e_{\xi,qp} + \mu_0 V^m_{\xi,qp}\right)\right]\text{d}V = \mathbf{i}^\dagger_{mq}\left(-i\mathbf{S}^\dagger_m\partial_\xi\mathbf{S}_m\right)\mathbf{i}_{mp} + i\mathbf{i}^\dagger_{mq}\left(\mathbf{I} - \mathbf{S}^\dagger_m\mathbf{S}_m\right)\partial_\xi\mathbf{i}_{mp}, \quad \text{(Equation 69)}$$

which can be summed over m to give the total integral over Ω^{node}. Finally, combining the results from Equations 65, 66, 68, and 69 allows us to compute the W-S matrix $\mathbf{Q}_\xi$.

RESOURCE AVAILABILITY

Lead contact

Requests for further information and resources should be directed to and will be fulfilled by the lead contact, Matthew R. Foreman (matthew.foreman@ntu.edu.sg).

Materials availability

This study did not generate new materials.

Data and code availability

- All data reported in this paper can be automatically generated using code deposited on GitHub.[65]

- All original code has been deposited on GitHub and is publicly available as of the date of publication.[65]
- Any additional information required to reanalyze the data reported in this paper is available from the lead contact upon request.

ACKNOWLEDGMENTS

N.B. was supported by Singapore Ministry of Education Academic Research Fund (Tier 1) grant RG66/23. M.R.F. was supported by funding from the Institute for Digital Molecular Analytics and Science (IDMxS) under the Singapore Ministry of Education Research Centres of Excellence scheme (EDUN C-33-18-279-V12) and by Nanyang Technological University grant SUG:022824-00001.

AUTHOR CONTRIBUTIONS

Conceptualization, M.R.F.; methodology, N.B. and M.R.F.; investigation, N.B.; writing – original draft, N.B. and M.R.F.; writing – review & editing, N.B. and M.R.F.; funding acquisition, M.R.F.; supervision, M.R.F.

DECLARATION OF INTERESTS

The authors declare no competing interests.

Received: February 3, 2025
Revised: April 19, 2025
Accepted: July 3, 2025

REFERENCES

1. Eleuch, H., and Rotter, I. (2017). Resonances in open quantum systems. Phys. Rev. *95*, 022117. https://doi.org/10.1103/PhysRevA.95.022117.
2. Kappos, A. (2014). Seismic Analysis of Concrete Bridges: Numerical Modeling. In Encyclopedia of Earthquake Engineering, M. Beer, I.A. Kougioumtzoglou, E. Patelli, and S.-K. Au, eds. (Springer Berlin Heidelberg), pp. 1–37. https://doi.org/10.1007/978-3-642-36197-5_127-1.
3. Gay-Balmaz, P., and Martin, O.J.F. (2002). Electromagnetic resonances in individual and coupled split-ring resonators. J. Appl. Phys. *92*, 2929–2936. https://doi.org/10.1063/1.1497452.
4. Zhao, W., Molin, B., Wang, Y., Wolgamot, H.A., and Taylor, P.H. (2022). Nonlinear harmonics of gap fluid resonance with floating body motions. J. Fluid Mech. *951*, A23. https://doi.org/10.1017/jfm.2022.834.
5. Krasnok, A., Baranov, D., Li, H., Miri, M.A., Monticone, F., and Alú, A. (2019). Anomalies in Light Scattering. Adv. Opt Photon *11*, 892–951. https://doi.org/10.1364/aop.11.000892.
6. Lalanne, P., Yan, W., Gras, A., Sauvan, C., Hugonin, J.P., Besbes, M., Demésy, G., Truong, M.D., Gralak, B., Zolla, F., et al. (2019). Quasinormal mode solvers for resonators with dispersive materials. J. Opt. Soc. Am. A *36*, 686–704. https://doi.org/10.1364/JOSAA.36.000686.
7. Schrödinger, E. (1926). Quantisierung als Eigenwertproblem. Ann. Phys. *385*, 437–490. https://doi.org/10.1002/andp.19263840404.
8. Brillouin, L. (1932). Les problèmes de perturbations et les champs self-consistents. J. Phys. Radium *3*, 373–389. https://doi.org/10.1051/jphysrad:jphysrad0193200309037300.
9. Kelly, H.P. (1964). Many-Body Perturbation Theory Applied to Atoms. Phys. Rev. *136*, B896–B912. https://doi.org/10.1103/PhysRev.136.B896.
10. Capitani, S. (2003). Lattice perturbation theory. Phys. Rep. *382*, 113–302. https://doi.org/10.1016/S0370-1573(03)00211-4.
11. Ashida, Y., Gong, Z., and Ueda, M. (2020). Non-Hermitian physics. Adv. Phys. X. *69*, 249–435. https://doi.org/10.1080/00018732.2021.1876991.
12. Rotter, S., and Gigan, S. (2017). Light fields in complex media: Mesoscopic scattering meets wave control. Rev. Mod. Phys. *89*, 015005. https://doi.org/10.1103/RevModPhys.89.015005.
13. Kristensen, P.T., Herrmann, K., Intravaia, F., and Busch, K. (2020). Modeling electromagnetic resonators using quasinormal modes. Adv. Opt Photon *12*, 612–708. https://doi.org/10.1364/AOP.377940.
14. Baranov, D.G., Krasnok, A., Shegai, T., Alù, A., and Chong, Y. (2017). Coherent perfect absorbers: linear control of light with light. Nat. Rev. Mater. *2*, 17064. https://doi.org/10.1038/natrevmats.2017.64.
15. Miri, M.A., and Alù, A. (2019). Exceptional points in optics and photonics. Science *363*, eaar7709. https://doi.org/10.1126/science.aar7709.
16. Hsu, C.W., Zhen, B., Stone, A.D., Joannopoulos, J.D., and Soljačić, M. (2016). Bound states in the continuum. Nat. Rev. Mater. *1*, 16048. https://doi.org/10.1038/natrevmats.2016.48.
17. Chen, C., and Wang, J. (2020). Optical biosensors: An exhaustive and comprehensive review. Analyst *145*, 1605–1628. https://doi.org/10.1039/C9AN01998G.
18. Degen, C.L., Reinhard, F., and Cappellaro, P. (2017). Quantum sensing. Rev. Mod. Phys. *89*, 035002. https://doi.org/10.1103/RevModPhys.89.035002.
19. Foreman, M.R., Swaim, J.D., and Vollmer, F. (2015). Whispering gallery mode sensors. Adv. Opt. Photonics *7*, 168–240. https://doi.org/10.1364/AOP.7.000168.
20. Ruesink, F., Doeleman, H.M., Hendrikx, R., Koenderink, A.F., and Verhagen, E. (2015). Perturbing Open Cavities: Anomalous Resonance Frequency Shifts in a Hybrid Cavity-Nanoantenna System. Phys. Rev. Lett. *115*, 203904. https://doi.org/10.1103/PhysRevLett.115.203904.
21. Azeem, F., Trainor, L.S., Devane, P.A., Norman, D.S., Rueda, A., Lambert, N.J., Kumari, M., Foreman, M.R., and Schwefel, H.G.L. (2021). Dielectric Perturbations: Anomalous Resonance Frequency Shifts in Optical Resonators. Opt. Lett. *46*, 2477–2480. https://doi.org/10.1364/OL.420791.
22. Parto, M., Liu, Y.G.N., Bahari, B., Khajavikhan, M., and Christodoulides, D.N. (2020). Non-Hermitian and topological photonics: optics at an exceptional point. Nanophotonics *10*, 403–423. https://doi.org/10.1515/nanoph-2020-0434.
23. Sternheim, M.M., and Walker, J.F. (1972). Non-Hermitian Hamiltonians, Decaying States, and Perturbation Theory. Phys. Rev. C *6*, 114. https://doi.org/10.1103/PhysRevC.6.114.
24. Ching, E.S.C., Leung, P.T., Maassen van den Brink, A., Suen, W.M., Tong, S.S., and Young, K. (1998). Quasinormal-mode expansion for waves in open systems. Rev. Mod. Phys. *70*, 1545–1554. https://doi.org/10.1103/RevModPhys.70.1545.
25. Vahala, K.J. (2003). Optical microcavities. Nature *424*, 839–846. https://doi.org/10.1038/nature01939.
26. Waldron, R.A. (1960). Perturbation theory of resonant cavities. Proc. IEE C. Monogr. UK. *107*, 272–274. https://doi.org/10.1049/pi-c.1960.0041.
27. Bethe, H.A., and Schwinger, J. (1943). Perturbation theory for cavities. N. D.R.C. Rpt. D1-117 (Cornell University).
28. Lalanne, P., Yan, W., Vynck, K., Sauvan, C., and Hugonin, J.P. (2018). Light interaction with photonic and plasmonic resonances. Laser Photon. Rev. *12*, 1700113. https://doi.org/10.1002/lpor.201700113.
29. Fyodorov, Y.V., and Savin, D.V. (2012). Statistics of resonance width shifts as a signature of eigenfunction nonorthogonality. Phys. Rev. Lett. *108*, 184101. https://doi.org/10.1103/PhysRevLett.108.184101.
30. Gros, J.B., Kuhl, U., Legrand, O., Mortessagne, F., Richalot, E., and Savin, D.V. (2014). Experimental width shift distribution: A test of nonorthogonality for local and global perturbations. Phys. Rev. Lett. *113*, 224101. https://doi.org/10.1103/PhysRevLett.113.224101.
31. Chen, P.Y., Bergman, D.J., and Sivan, Y. (2019). Generalizing Normal Mode Expansion of Electromagnetic Green's Tensor to Open Systems. Phys. Rev. Appl. *11*, 044018. https://doi.org/10.1103/PhysRevApplied.11.044018.
32. Byrnes, N., and Foreman, M.R. (2025). Generalized Wigner-Smith analysis of resonance perturbations in arbitrary *Q* non-Hermitian systems. Phys. Rev. Research *7*, 013299. https://doi.org/10.1103/PhysRevResearch.7.013299.

33. Texier, C. (2016). Wigner time delay and related concepts: Application to transport in coherent conductors. Phys. E Low-dimens. Syst. Nanostruct. *82*, 16–33. https://doi.org/10.1016/j.physe.2015.09.041.

34. Patel, U.R., and Michielssen, E. (2021). Wigner–Smith Time-Delay Matrix for Electromagnetics: Theory and Phenomenology. IEEE Trans. Antenn. Propag. *69*, 902–917. https://doi.org/10.1109/TAP.2020.3008650.

35. de Carvalho, C.A.A., and Nussenzveig, H.M. (2002). Time delay. Phys. Rep. *364*, 83–174. https://doi.org/10.1016/S0370-1573(01)00092-8.

36. Mao, Y., Patel, U.R., and Michielssen, E. (2023). Wigner–Smith Time Delay Matrix for Electromagnetics: Systems With Material Dispersion and Losses. IEEE Trans. Antenn. Propag. *71*, 5266–5275. https://doi.org/10.1109/TAP.2023.3262979.

37. Ambichl, P., Brandstötter, A., Böhm, J., Kühmayer, M., Kuhl, U., and Rotter, S. (2017). Focusing inside Disordered Media with the Generalized Wigner-Smith Operator. Phys. Rev. Lett. *119*, 033903. https://doi.org/10.1103/PhysRevLett.119.033903.

38. Horodynski, M., Kühmayer, M., Brandstötter, A., Pichler, K., Fyodorov, Y. V., Kuhl, U., and Rotter, S. (2019). Optimal wave fields for micromanipulation in complex scattering environments. Nat. Photonics *14*, 149–153. https://doi.org/10.1038/s41566-019-0550-z.

39. Bouchet, D., Rotter, S., and Mosk, A.P. (2021). Maximum information states for coherent scattering measurements. Nat. Phys. *17*, 564–568. https://doi.org/10.1038/s41567-020-01137-4.

40. Horodynski, M., Kühmayer, M., Ferise, C., Rotter, S., and Davy, M. (2022). Anti-reflection structure for perfect transmission through complex media. Nature *607*, 281–286. https://doi.org/10.1038/s41586-022-04843-6.

41. Trefethen, L., and Bau, D. (1997). Numerical Linear Algebra (SIAM). https://doi.org/10.1137/1.9781611977165.

42. Binkowski, F., Betz, F., Hammerschmidt, M., Schneider, P.I., Zschiedrich, L., and Burger, S. (2022). Computation of eigenfrequency sensitivities using Riesz projections for efficient optimization of nanophotonic resonators. Commun. Phys. *5*, 202. https://doi.org/10.1038/s42005-022-00977-1.

43. Fyodorov, Y.V., and Sommers, H.J. (1997). Statistics of resonance poles, phase shifts and time delays in quantum chaotic scattering: Random matrix approach for systems with broken time-reversal invariance. J. Math. Phys. *38*, 1918–1981. https://doi.org/10.1063/1.531919.

44. Weiss, T., and Muljarov, E.A. (2018). How to calculate the pole expansion of the optical scattering matrix from the resonant states. Phys. Rev. B *98*, 085433. https://doi.org/10.1103/physrevb.98.085433.

45. Othonos, A. (1997). Fiber Bragg gratings. Rev. Sci. Instrum. *68*, 4309–4341. https://doi.org/10.1063/1.1148392.

46. Gaio, M., Saxena, D., Bertolotti, J., Pisignano, D., Camposeo, A., and Sapienza, R. (2019). A nanophotonic laser on a graph. Nat. Commun. *10*, 226. https://doi.org/10.1038/s41467-018-08132-7.

47. (2007). Ring resonators: Theory and modeling. In Integrated Ring Resonators: The CompendiumIntegrated Ring Resonators: The Compendium (Springer Berlin Heidelberg), pp. 3–40. https://doi.org/10.1007/978-3-540-68788-7_2.

48. Geyi, W. (2019). Stored electromagnetic field energies in general materials. J. Opt. Soc. Am. B *36*, 917–925. https://doi.org/10.1364/JOSAB.36.000917.

49. Xiao, Y.F., Liu, Y.C., Li, B.B., Chen, Y.L., Li, Y., and Gong, Q. (2012). Strongly enhanced light-matter interaction in a hybrid photonic-plasmonic resonator. Phys. Rev. *85*, 031805. https://doi.org/10.1103/PhysRevA.85.031805.

50. Hu, Y., Shao, L., Arnold, S., Liu, Y.C., Ma, C.Y., and Xiao, Y.F. (2014). Mode broadening induced by nanoparticles in an optical whispering-gallery microcavity. Phys. Rev. *90*, 043847. https://doi.org/10.1103/PhysRevA.90.043847.

51. Betz, F., Hammerschmidt, M., Zschiedrich, L., Burger, S., and Binkowski, F. (2024). Efficient Rational Approximation of Optical Response Functions with the AAA Algorithm. Laser Photon. Rev. *18*, 2400584. https://doi.org/10.1002/lpor.202400584.

52. Saxena, D., Fischer, A., Dranczewski, J., Ng, W.K., Trivino, N.V., Schmid, H., Raziman, T.V., Arnaudon, A., Barahona, M., Hess, O., et al. (2025). Designed Semiconductor Network Random Lasers. Laser & Photonics Reviews *n/a*. Laser Photon. Rev. *19*, 2400623. https://doi.org/10.1002/lpor.202400623.

53. Wang, X.S., Savo, R., Maeder, A., Kaufmann, F., Kellner, J., Morandi, A., Rotter, S., Sapienza, R., and Grange, R. (2023). Graph model for multiple scattering in lithium niobate on insulator integrated photonic networks. Opt. Express *31*, 42255–42270. https://doi.org/10.1364/oe.492431.

54. Giacomelli, G., Lepri, S., and Trono, C. (2019). Optical networks as complex lasers. Phys. Rev. *99*, 023841. https://doi.org/10.1103/physreva.99.023841.

55. Polyanskiy, M.N. (2024). Refractiveindex.info database of optical constants. Sci. Data *11*, 94. https://doi.org/10.1038/s41597-023-02898-2.

56. Byrnes, N., and Foreman, M.R. (2022). Polarisation statistics of vector scattering matrices from the circular orthogonal ensemble. Opt. Commun. *503*, 127462. https://doi.org/10.1016/j.optcom.2021.127462.

57. Chong, Y.D., Ge, L., Cao, H., and Stone, A.D. (2010). Coherent perfect absorbers: Time-reversed lasers. Phys. Rev. Lett. *105*, 053901. https://doi.org/10.1103/PhysRevLett.105.053901.

58. Andreasen, J., Asatryan, A.A., Botten, L.C., Byrne, M.A., Cao, H., Ge, L., Labonté, L., Sebbah, P., Stone, A.D., Türeci, H.E., and Vanneste, C. (2010). Modes of random lasers. Adv. Opt Photon *3*, 88. https://doi.org/10.1364/aop.3.000088.

59. Bachelard, N., Andreasen, J., Gigan, S., and Sebbah, P. (2012). Taming random lasers through active spatial control of the pump. Phys. Rev. Lett. *109*, 033903. https://doi.org/10.1103/PhysRevLett.109.033903.

60. Bachelard, N., Gigan, S., Noblin, X., and Sebbah, P. (2014). Adaptive pumping for spectral control of random lasers. Nat. Phys. *10*, 426–431. https://doi.org/10.1038/nphys2939.

61. Granchi, N., Intonti, F., Florescu, M., García, P.D., Gurioli, M., and Arregui, G. (2023). Q-Factor Optimization of Modes in Ordered and Disordered Photonic Systems Using Non-Hermitian Perturbation Theory. ACS Photonics *10*, 2808–2815. https://doi.org/10.1021/acsphotonics.3c00510.

62. Hjørungnes, A. (2011). Complex-Valued Matrix Derivatives: With Applications in Signal Processing and Communications (Cambridge University Press). https://doi.org/10.1017/CBO9780511921490.

63. Ahlfors, L. (1979). Complex Analysis: An Introduction to the Theory of Analytic Functions of One Complex Variable (McGraw-Hill Education).

64. Snyder, A., and Love, J. (2012). Optical Waveguide Theory (New York: Springer). https://doi.org/10.1007/978-1-4613-2813-1.

65. Byrnes, N., and Foreman, M.R. (2025). generalized-wigner-smith-high-q. https://github.com/Optical-Theory-Group/generalized-wigner-smith-high-Q.GitHub.